Preparation and characterization of cross-linked polymer supports for catalysts immobilization

Maria P. Bracciale[1], Alessandra Broggi[2*], Elena Bartollini[3], Francesca Sbardella[4], Matteo Poldi[5], Assunta Marrocchi[6*], Maria L. Santarelli[7*], Luigi Vaccaro[8*]

[1,2,4,5,7]Dipartimento di Ingegneria Chimica Materiali Ambiente, Università di Roma "La Sapienza", Via Eudossiana 18, 00185 Roma, Italy;

[3,6,8]Laboratory of Green Synthetic Organic Chemistry, Dipartimento di Chimica, Università degli Studi di Perugia, Via Elce di Sotto 8, 06123 Perugia, Italy.

Abstract— *A series of macroporous cross-linked polystyrenes for applications as supports in catalysis have been synthesized and characterized in terms of their structural, thermal and morphological features. In this regards, we have shown how Fourier-transformed infrared spectroscopy mapping (μ-FTIR) may represent a very useful and easy-to-handle tool for the advanced spatial characterization of substituted cross-linked resins at a single bead level, thereby helping synthetic chemists in the prediction of their behavior during chemical processes. Further, scanning electron microscopy (SEM), thermal analysis (MTDSC), and N_2 absorption (BET) measurements have been performed. Direct correlations between the polymerization conditions and resins chemical-physical properties have been identified.*

Keywords— Polymer catalyst supports; Green Chemistry; macroporous resins; polystyrene; micro-FTIR

I. INTRODUCTION

Catalysis underpins the chemical/petrochemical industry, being fundamental to the chemical production, e.g. fuels, plastics, etc. Indeed, around 90 percent of chemical manufacturing processes use catalysis to enhance production efficiency and reduce energy use, thereby reducing, in turn, greenhouse gas emissions. [1] Currently, the general trend in catalysis is the engineering of heterogeneous systems that should allow the recovery and reuse of the catalyst [2-5], therefore solving the crucial economic issues as well as environmental concerns. The usually high catalyst cost can be affordable in commercial applications only when the productivity of the catalyst, measured as total kg of products produced per kg of catalyst, is high enough to make the chemical process economically viable.

Besides, the principles of Green Chemistry (or Sustainable Chemistry) [6] express the need of industry to make maximum efforts to minimize waste, particularly if containing toxic/exhaustive metals such as those typically present in transition metal catalytic systems [7]. In this regard, over the past decades a large number of catalysts have been supported on a variety of materials ranging from inorganic/organic polymers to mesoporous silica [1-5].

Catalyst supports based on organic insoluble (cross-linked) polymers are arguably among the most versatile supports in the literature [1-5]. In particular, insoluble polymers supports are advantageous since, for instance, several catalysts immobilized on the insoluble matrix show enhanced stability to hydrolysis and oxidation, they are easier to handle, and generally give purer products in chemical processes. Further, the development of highly functional group tolerant controlled and living polymerization methods [8-14] has allowed for the tuning of the structure and density of catalyst sites along polymers and the easy incorporation of catalyst into polymer structures. Nevertheless, the use of insoluble polymers presents some drawbacks, such as lower activities and selectivities when compared with their non-supported analogues. Diffusion effects, accessibility of the catalytic sites by the reagents in solution, and site heterogeneity might be considered in part responsible for these results [1-5, 15-16]. In this regards, the availability of analytical tools enabling the determination of functional groups distribution and accessibility of reagents, which can be of simple and general use, is rather limited.

We have contributed [17-21] to the development of sustainable and efficient procedures based on the use of metal-free catalysts supported on macroporous cross-linked copolymers of 4-vinylbenzylchloride with divinylbenzene [22]. While often successful in the recycling as well as the easy separation from the reaction mixtures, the use of such supported catalytic systems led, in some cases, to the occurrence of slow reactions and poor yields.

The objective of the present paper is to provide an informed picture of the synthesis-structure-morphology correlation in a wide set of such resins, and, ultimately, to help overcome failures experienced with attempts to use some polymer supports.

Particularly, herein we show how Fourier transformed infrared micro-spectroscopy (μ-FTIR) technique [23-24] can become a very useful tool for the routine analysis of polymer-supported catalysts, to examine functional groups distribution and accessibility of reagents at a *single-bead level*. Indeed, most efforts in examining the properties of solid supports focus on surface area, porosity and swelling of the beads, whereas relatively little attention has been given to the site of functionalization. Heterogeneous micro-domains within a bead can yield important consequences for the macroscopic properties (e.g. swelling) [25], and can lead to inhomogeneous reactivity of functional groups within a region of a bead.

To the best of our knowledge, up to now only one relevant report has dealt with the feasibility of using μ-FTIR to examine insoluble polymer catalyst supports. Indeed, in 2004, Mandair et al. [24] successfully exploited this technique on flattened resin beads.

We report for the first time the use of IR reflectance mapping to provide direct evidence for the homogeneity of resin beads in their original spherical form. No flattening is useful when quantifying species immobilized on highly cross-linked resin beads since these latter shatter if compressed.

Further, we present the resins characterization by scanning electron microscopy (SEM), and measuring the pore size, surface area, and thermal decomposition temperature. Trends in the resin surface area and porosity are identified and analyzed.

II. RESULTS AND DISCUSSION

2.1 Resins preparation.

The synthesis of resins **1*a*-*o*** was performed by α,α′-azoisobutyronitrile (AIBN)-initiated suspension copolymerization of vinylbenzylchloride (**2**) and divinylbenzene (**3**) mixture using 2-ethyl-hexanoic acid (2-EHA), 1-chlorodecane (1-CD), and cyclohexanol (COX) as porogens (or pore-formers) (Scheme 1).

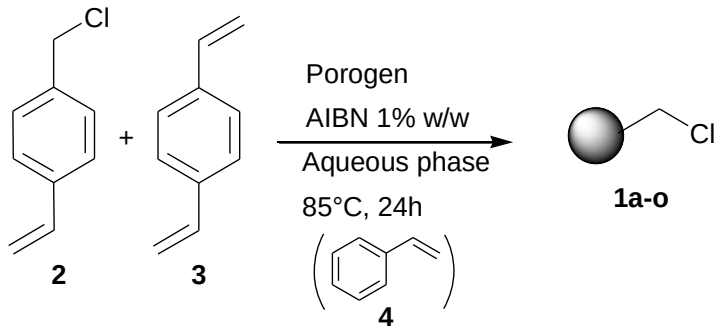

SCHEME 1. SYNTHESIS OF PS-Cl RESINS 1*a*-*o*

In the case of **1*h*** and **1*m***, styrene co-monomer was added in low percentage (2% and 4%, respectively) to modulate the resins chloromethyl content (Scheme 1 and Table 1). The required porogens were selected bearing in mind their effectiveness [26-31] in generating macroporous structures. Moreover, the choice of three chemically different porogen (acidic, polar protic, polar aprotic) was made to identify a correlation between support characteristics and the nature of the porogen.

The polymerization yields were generally good (65-78%, Table 1) and in agreement with the expected values. For all the porogens, when a low concentration (0.1%) of poly(vinyl alcohol) (PVA1) stabilizer (MW 13.000-23.000) was used, powdered/scaled products were obtained (Table 1).

In the case of 2-EHA porogen, the use of high-molecular weight PVA4 stabilizer (MW 85.000-124.000) gave spherical beaded products for both stabilizer concentrations (0.1% and 0.4%). When COX and 1-CD porogens were used, a low concentration of stabilizer (PVA1 or PVA4) always led to powdered or scaled resins. On the other hand, in the case of COX, spherical beaded products were obtained with high concentration (0.4%) of PVA4 provided that a different VBC/S/DV (4-vinylbenzylchloride/styrene/divinylbenzene) co-monomer ratio of 0.6/0/0.4 or 0.6/0.2/0.2 was used (entries 8 and 9, Table 1). In the case of **1*a*-*b***, **1*h*-*n***, (i.e. spherical beaded products) typical average bead diameters in the range of 25-100 μm were obtained. Importantly, a narrow size distribution of the beads within each resin was achieved. Indeed, size distribution is often a critical factor for high quality synthesis supports [32]. The use of cyclohexanol generated the smallest particle (average size ~100 μm).

TABLE 1

POLYMERS 1*a-o* FEATURES AND SYNTHESIS CONDITION[a]

Entry	Polymer	Stabilizer (%)	Porogen	VBC/S/DV	Yields (%)	Physical format
1	**1*a***	PVA4 (0.1)	2-EHA	0.8/0/0.2	72	beads
2	**1*b***	PVA4 (0.4)	2-EHA	0.8/0/0.2	75	beads
3	**1*c***	PVA1 (0.1)	2-EHA	0.8/0/0.2	68	powder
4	**1*d***	PVA1 (0.4)	2-EHA	0.8/0/0.2	70	powder
5	**1*e***	PVA1 (0.1)	COX	0.8/0/0.2	65	powder
6	**1*f***	PVA4 (0.1)	COX	0.8/0/0.2	70	scales
7	**1*g***	PVA4 (0.4)	COX	0.8/0/0.2	71	powder
8	**1*h***	PVA4 (0.4)	COX	0.6/0.2/0.2	78	beads
9	**1*i***	PVA4 (0.4)	COX	0.6/0/0.4	73	beads
10	**1*j***	PVA1 (0.4)	COX	0.8/0/0.2	65	beads
11	**1*k***	PVA4 (0.1)	1-CD	0.8/0/0.2	71	scales
12	**1*l***	PVA4 (0.4)	1-CD	0.8/0/0.2	68	beads
13	**1*m***	PVA4 (0.4)	1-CD	0.4/0.4/0.2	75	beads
14	**1*n***	PVA1 (0.4)	1-CD	0.8/0/0.2	70	beads
15	**1*o***	PVA1 (0.1)	1-CD	0.8/0/0.2	70	powder

[a]PVA1= poly(vinyl alcohol) (MW 13.000-23.000); PVA4= poly(vinyl alcohol) (MW 85.000-124.000); 2-EHA= 2-ethylhexanoic acid; COX= cyclohexanol; 1-CD= 1-chlorodecane; VBC/S/DV= 4-vinyl benzyl chloride/styrene/divinylbenzene

Note here that powders are not preferred in many large-scale applications, owing to dusting problems and excessive pressure drops across the catalyst in fixed-bed reactors [33]. Further, irregularly shaped (e.g. scaled resins) particles may be susceptible to mechanical attrition, and breakdown to "fines" [34]. Therefore resins **1*c-g***, **1*k***, **1*o*** were not investigated further

2.2 Resins characterization

The FTIR spectra of resins **1*a-b*** and **1*h-n*** are reported in Figure 1 and Figures SI1-7.

In all cases, they exhibited a series of strong peaks at 1421cm^{-1} and 675 cm^{-1}, which were attributed to the characteristic absorptions of the chloromethyl group –CH_2Cl. The band at 675 cm^{-1} corresponds to the stretching vibration of C–Cl bond, and the band at 1421 cm^{-1} is corresponding to the bending vibration of -CH_2 in –CH_2Cl. Besides, the IR spectra exhibited two peaks at 1265 cm^{-1}and 823 cm^{-1}, which were attributed to the vibration absorptions of =C–H bond of the –CH_2Cl *p*-substituted benzene rings [35].The band at ~3300 cm^{-1} corresponds to the presence of a low degree of hydroxyl groups content in the resins. This might be explained by the partial hydrolysis of the chloromethylene groups in vinylbenzene chlorides. Indeed, suspension polymerizations are carried out at elevated temperatures in the presence of excess water, and it is not therefore surprising that this side reaction occurs [36-39].

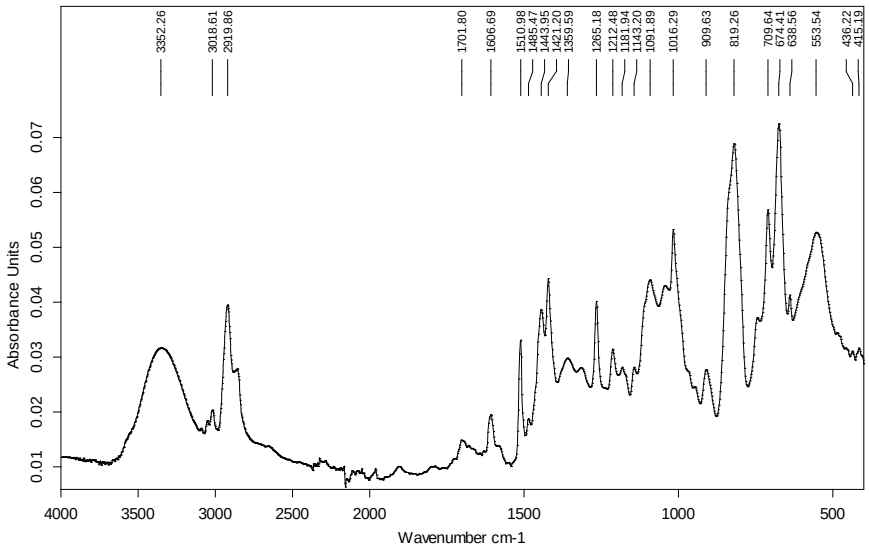

FIGURE 1. FTIR ANALYSIS OF POLYMER 1*a*

To demonstrate the effective distribution of –Cl groups on chloromethylated polystyrene resin beads, a μ-FTIR analysis (Fourier transformed infrared micro-spectroscopy) [23-24] was performed (see also Experimental Section).

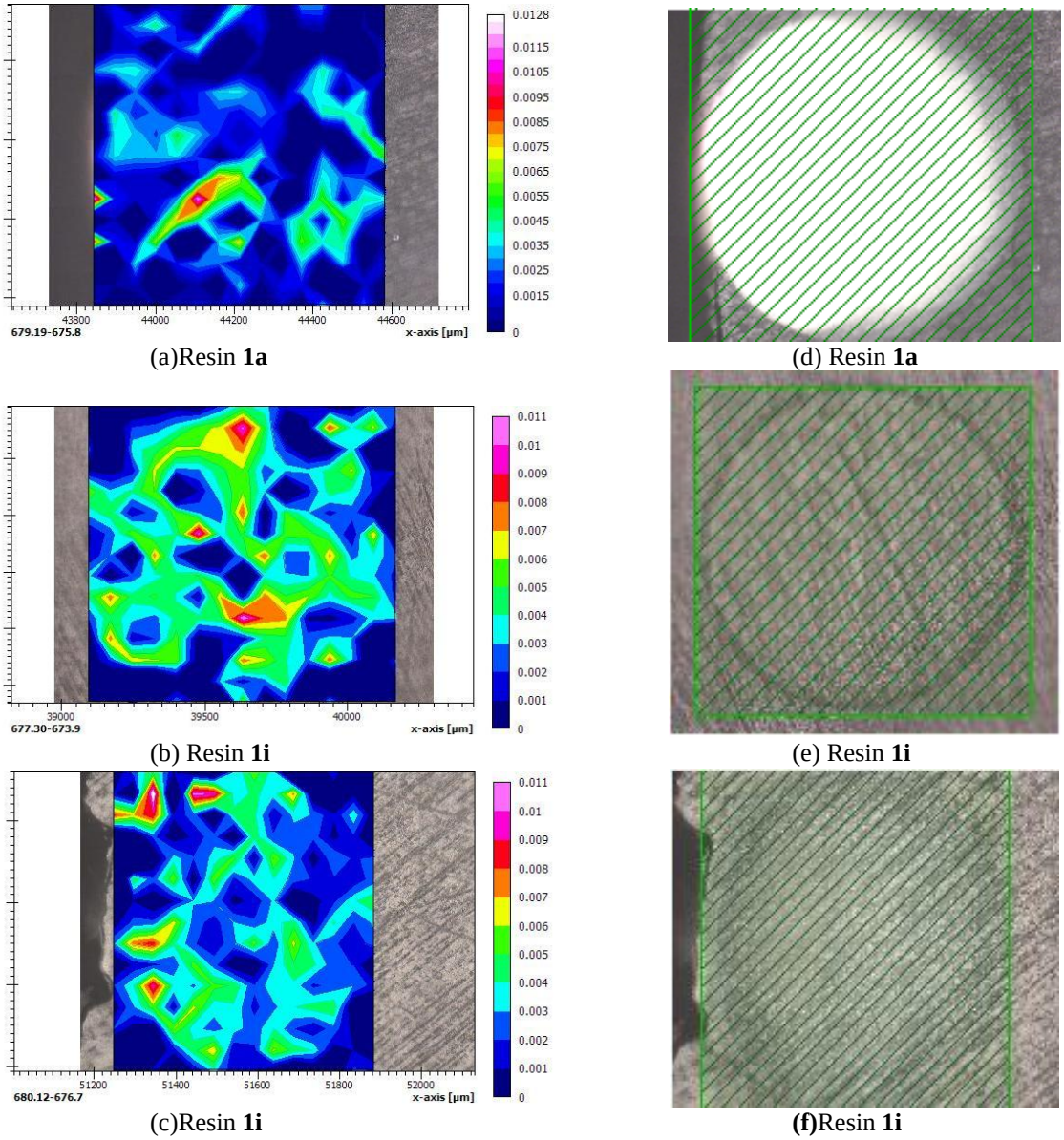

FIGURE 2. SPECTROSCOPIC 2D IMAGES OF THE SPATIAL DISTRIBUTION OF–CL GROUPS (A-C). OPTICAL MICROSCOPY IMAGES 15X (D-F) SHOWING THE HALF-CUT BEAD MAPPING TRACE. ALL SPECTRA WERE COLLECTED IN REFLECTION MODE WITH A 3 cm^{-1} SPECTRAL RESOLUTION, AND THE IMAGES WERE OBTAINED BY MONITORING THE PEAK CENTRED AT 675 cm^{-1}; THE ABSORPTION INTENSITY WAS MEASURED AND EXPRESSED AS ARBITRARY UNITS.

In order to observe the active site spatial distribution, the peak centered at 675 cm^{-1} (i.e. C–Cl stretching vibration frequency) was monitored throughout the half-cut resin beads (Figure 2 and SI8). The resulting 2D images (Figures 2a-c and Figures SI8a-e) indicated that the spatial distribution of -Cl groups is generally regular and homogeneous for samples deriving from the use of a high concentration (0.4%) of PVA stabilizer (Figures 2b-c and Figures SI8a-e). Further, a better homogeneity in –Cl distribution may be generally observed for samples prepared through the use of high-molecular weight PVA4 compared to PVA 1stabilizer, as exemplified in Figure 2b (resin **1*i***) and Figure 2c (resin **1*n***), respectively.

Next, we also performed nucleophilic substitution of the chlorine atoms in the representative resin **1*l*** by 1,5,7-triazabicyclo[4.4.0]dec-5-ene (TBD) base in dioxane at 60°C [20]. The μ-FTIR analysis of the resulting catalytic system actually demonstrated a regular and homogeneous distribution of TBD active sites. The most obvious evidence of this was

the disappearance of the chloromethyl band at 675 cm^{-1} and the appearance of the C-N band at 1370 cm^{-1} (i.e. C-N stretching vibration frequency) (Figures SI9-10) on the overall bead surface [17]. These findings anticipated a good site accessibility for resin 1*l*, thereby further pointing out the utility of such analytical technique.

The micro analytical data (C, H) obtained from elemental analysis indicated contents of carbon and hydrogen in a range of 72.98-81.07% and 6.42-7.44% respectively, which correspond to a resin chlorine content (*loading*) in the range 3.09-4.73 mmol/g.

Brunauer–Emmett–Teller (BET) [32] analyses were performed to determine surface area, average pore volume, average pore size, and pore size distribution (Table 2 and Figure SI11-18). A direct correlation [31,34] may be observed for resins through 1-chlorodecane porogen (entries 12-14, Table 2). Indeed, when PVA4 is used in the case of polymers **1*l*** and **1*m*** (entries 12-13, Table 2), high values of surface area were obtained (107.1 m^2/g and 78.3 m^2/g, respectively). When PVA1 at the same concentration (0.4%) is used, polymer **1*n*** (entry 14) resulted in a low value surface area (24.6 m^2/g). In the case of cyclohexanol porogen (entries 8-10, Table 2), when PVA1 is used (resin **1*j***) the highest average pore size was achieved (107 Å and 396 Å, respectively). On the other hand, resins **1*i*** prepared by employing high-molecular weight PVA4, gave lower average pore radius and average pore volume (entry 9 *vs* 10, Table 2).

This finding indicated that despite an excellent distribution of –Cl groups (Figure 2b), resin **1*i*** may feature a scarce accessibility of the active sites by solvents/reagents when used as catalyst support, thereby leading to a reduced efficiency of the catalyst itself.

TABLE 2

SOLID-STATE POROSITY DATA OF POLYMERS 1*a-b* and **1*h-n***

Entry	Polymer	Surface area (m^2/g)	Average pore volume (cm^3/g)	Average pore radius (Å)
1	**1*a***	5.0	0.0188	77
2	**1*b***	27.2	0.29	85
8	**1*h***	3.4	0.02	107
9	**1*i***	0.3	10^{-3}	8
10	**1*j***	23.0	0.21	396
12	**1*l***	107.1	0.31	116
13	**1*m***	78.3	0.54	137
14	**1*n***	24.6	0.11	91

In the case of resins prepared with 2-EHA as porogen (entries 1 and 2, Table 1), low surface area (5.0 m^2/g and 27.2 m^2/g, respectively) and average pore radius (77 Å and 85 Å, respectively) were observed. 1-CD and COX revealed to be the best porogens in terms of average pore size and surface area, respectively, thereby suggesting the easiest accessibility to functional –Cl groups. Indeed, porogen effects on pore structure and surface area are well-known [40-41]. A rather large population of mesopores (1.6-33.3 nm) has been generally observed (Figures SI11-18), except for **1*i***, thereby indicating that all the porogens are thermodinamically compatible with the polymer matrix and/or the cross-linker percentage [32]. The smaller types of pore are essential to a high surface area [32].

The resins **1*a-b*** and **1*h-n*** were subjected to modulated temperature differential scanning calorimetry (MTDSC) analysis, showing high thermal stability in the range of 30-250°C (Figure 3 and Figures SI19-25). Particularly, MTDSC plot for **1*n*** reveals a rearrangement of the crystalline structure for this latter (so-called *secondary transitions*) occurring at ~220°C (Figure 3).

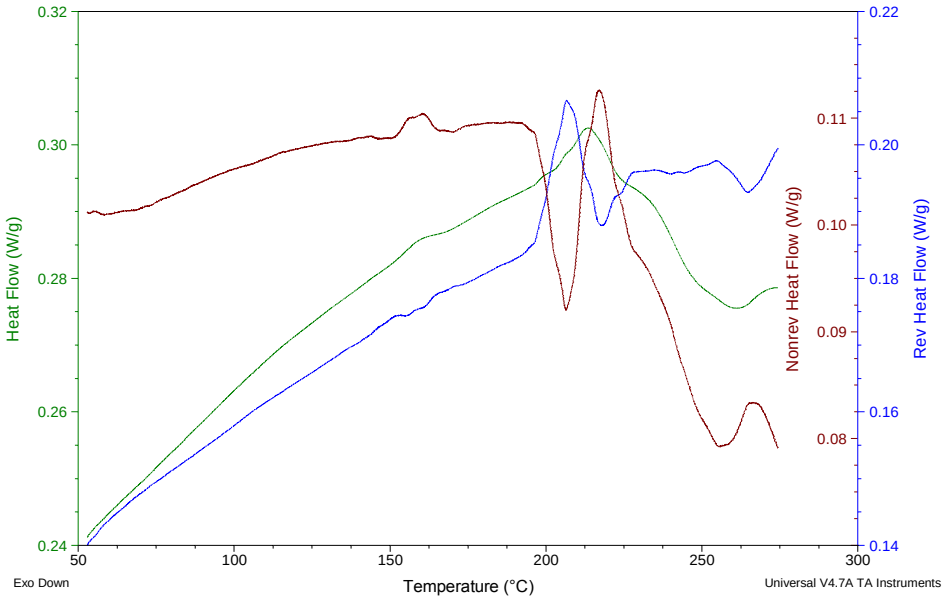

FIGURE 3. MTDSC ANALYSIS OF POLYMER 1*n*

Scanning electron microscopy (SEM) was used to investigate polymers' surface morphology and particle size (Figures SI26-27). Resins **1*a***, **1*h***, **1*m*** and **1*n*** (Figures SI26a, SI26c, SI27c and SI27d, respectively) reveal a clear macropores population even at the bead surface. Resins **1*b***, **1*j*** and **1*l*** (Figures SI26b, SI27a and SI27b, respectively) showed rough contaminated surfaces with fragments associated with them or cracks. The contamination is however superficial, as the high-magnification SEM images of these resins show access to a discrete macroporous structure (Figures SI26f, SI27e and SI27f). Resin **1*i*** (Figure SI26d), however, shows a fine surface texture, which is rather uniform. SEM images of polymer fracture sections clearly show in all cases the formation of a typical macroporous structure (Figures SI26e-h and SI27e-h).

III. EXPERIMENTAL SECTION

3.1 General.

All the commercially available chemicals were purchased at Sigma–Aldrich and used without any further purification, unless otherwise noted. 4-vinylbenzylchloride (**2**), divinylbenzene (**3**) (80% grade) and styrene (**4**) (Scheme 1) were extracted three times with a 5% w/w NaOH solution to remove the polymerization inhibitor (tert-butyl catechol). □α, α ′-Azoisobutyronitrile (AIBN) was re-crystallized from methanol. Suspension polymerizations were run using a three-neck cylinder-shaped glass vessel, equipped with a mechanical stirrer, condenser, and nitrogen inlet [17]. Elemental microanalyses were performed using a Fison's EA1106 CHN analyzer using atropine, 2,5-bis-2-(5-tert-butylbenzoxazolyl) thiophene (BBOT) and phenanthrene as reference standard, with an accuracy of ca. 2 μmol/g.

Conventional FTIR spectra were recorded on a VERTEX 70 Bruker Optics instrument, spectral range 4000–400 cm^{-1}, resolution 4 cm^{-1}, equipped with single reflection diamond ATR cell.

μ-FTIR imaging was performed using a FT-IR microspectrometer Hyperion 2000 (Bruker Optics GmbH) equipped with a liquid nitrogen cooled MCT detector, in order to get the better signal to noise ratio. The microscope is equipped with a standard 15x objective. For μ-FTIR imaging, spectra were collected, in reflection mode, in the mid-infrared (MIR) range of 600–4000 cm^{-1} at a resolution of 3 cm^{-1} with 128 co-added scans. Sample step was 50 nm. All the data collection and processing were performed using OPUS 7.0 (Bruker). The measurements were carried out on half-cut resin beads after embedding in an acrylic resin support (TECHNOVIT 4004, Kulzer), and polishing with conventional methods using silicon carbide papers with grit 600, 1200 to 2500 (Buehler). The final polishing was attained using a polishing cloth.

Brunauer–Emmett–Teller (BET) analyses were performed by using an Autosorb iQ-MP/MPXR instrument (Quantachrome). Modulated temperature differential scanning calorimetry analysis (MTDSC) were performed with a TA instruments 2920 calorimeter with modulated cell cooled by nitrogen flow. Samples were analyzed in opened capsules with heating rate of 10 °C/min, ±0.5 °C modulation and 60s period.

Scanning electron microscopy (SEM) analyses were performed using an Auriga Zeiss HR FESEM instrument. SEM imaging of the surfaces of resin samples was performed with accelerating voltages between 5 keV and 30 keV, achieving magnifications ranging from 100x to 200kx.

3.2 Typical procedure for the preparation of chloromethylated resins PS-Cl 1.

The procedure for the synthesis of chloromethylated resin **1*a*** is reported as an example. Details on the reaction conditions for the remaining investigated **PS-Cl 1** are reported in the Supporting Information.

PS-Cl 1*a*. A reaction vessel immersed in an oil bath, equipped with condenser, mechanical stirrer and nitrogen inlet/outlet was charged with water (80 mL), poly(vinyl alcohol) (MW 85,000–124,000, 99% hydrolyzed) (0.1%), and NaCl (2.65 g) and stirred for 24 h at room temperature. A mixture of 4-vinylbenzylchloride (**2**), (1.6 mL), divinylbenzene (**3**) (0.4 mL), 2-ethylhexanoic acid (2-EHA, 2 mL) and AIBN (0.02 g, 1% w/w monomers) was then added into the reactor. The system was kept under stirring and purged with nitrogen for 30 min. Then, the reaction was warmed up to 85 °C under mechanical stirring. After 24 h, the reaction was allowed to reach room temperature and the polymer beads were filtered. The product was washed in a Soxhlet extractor for 24 h with water, THF and hexanes and vacuum dried overnight (yield 72%).

IV. CONCLUSION

To sum up, a new series of uniformly functionalized macroporous cross-linked resins to be employed as heterogeneous catalyst supports have been synthesized and characterized in terms of structure, thermal properties, and morphology. In order to obtain spherical-beaded products, in the case of 2-ethylhexanoic acid (2-EHA) porogen the use of high-molecular weight stabilizer is required, independently from its concentration. On the other hand, it was found that when cyclohexanol (COX) or 1-chlorodecane (1-CD) porogens are used, the presence of higher PVA concentration is needed, regardless of the stabilizer molecular weight. The relative ratio of all components, i.e. co-monomers, porogen, and stabilizer, allowed broad variation in the (micro) structure of the materials.

We showed for the first time that Fourier transformed infrared micro-spectroscopy (μ-FTIR) technique can be a powerful tool for the simple analysis of polymer supports as well as the corresponding immobilized catalytic systems, to examine functional groups distribution and accessibility of reagents at a *single-bead level*. This is of particular interest since it helps in the prediction of resin reactivity and behavior during solid phase synthesis.

Further, we found that the investigated resins feature high average pore size (except **1i**), thereby supporting an easy accessibility to functional –Cl groups.

ACKNOWLEDGEMENTS

This research has been developed and partially financed within the National project "BIT3G" – Italian Green Chemistry Cluster.

We gratefully acknowledge the Università degli Studi di Perugia, and the Ministero dell'Istruzione, dell'Università e della Ricerca (MIUR) for the financial support within the program "Firb-Futuro in Ricerca" ref. N. RBFR08JKHI. Furthermore, the author thanks Dr. Francesco Mura, Sapienza Nanoscience & Nanotechnology Laboratories (CNIS-SSN-Lab), for his helpful assistance in SEM analyses.

REFERENCES

[1] IEA, ICCA, and DECHEMA 2013. Technology Roadmap "Energy and GHG Reductions in the Chemical Industry via Catalytic Processes".
[2] N. Madhavan, C.W. Jones, and M. Weck, "Rational Approach to Polymer-Supported Catalysts: Synergy between Catalytic Reaction Mechanism and Polymer Design". *Acc. Chem. Res.* vol. 41, pp 1153-65, 2008.
[3] C. Baleizao, and H. Garcia, "Chiral Salen Complexes: An Overview to Recoverable and Reusable Homogeneous and Heterogeneous Catalysts". *Chem. Rev.* vol. 106, pp. 3987-43, 2006.
[4] P. Barbaro, "Recycling Asymmetric Hydrogenation Catalysts by Their Immobilization onto Ion-Exchange Resins". *Chemistry European J.* vol. 12, pp. 5666-75, 2006.
[5] J.M. Notestein, A. Katz, "Enhancing Heterogeneous Catalysis through Cooperative Hybrid Organic–Inorganic Interfaces". *Chemistry European J.* vol. 12 pp. 3954-65, 2006.
[6] P.T. Anastas, and J.C. Warner, *Green Chemistry: Theory and Practice.* Oxford University Press. New York, 1998.
[7] EuCheMS - European Association for Chemical and Molecular Sciences EuCheMS. 2011. *Chemistry-Developing solutions in a changing world*, Brussel.

[8] V.Sciannamea, R.Jérôme, and C. Detrembleur, "In-Situ Nitroxide-Mediated Radical Polymerization (NMP) Processes: Their Understanding and Optimization". *Chem. Rev.* vol. 108, pp. 1104-26,2008.
[9] N.V. Tsarevsky, and K. Matyjaszewski, "Green Atom Transfer Radical Polymerization: From Process Design to Preparation of Well-Defined Environmentally Friendly Polymeric Materials". *Chem. Rev.* vol. 107, pp. 2270-99, 2007.
[10] C. Barner-Kowollik, T.P. Davis, J.P.A. Heuts, M.H. Stenzel, P.Vana, and M. Whittaker, "RAFTing down under: Tales of missing radicals, fancy architectures, and mysterious holes". *J. Polym. Sci. Polym. Chem.* vol. 41, pp. 365-75, 2003.
[11] M. Kamigaito, T. Ando, and M. Sawamoto,. "Metal-Catalyzed Living Radical Polymerization". *Chem. Rev.* vol. 101, pp. 3689-45, 2001.
[12] C.J. Hawker, "Living Free Radical Polymerization: A Unique Technique for the Preparation of Controlled Macromolecular Architectures". *Acc. Chem. Res.* vol. 30, pp. 373-382, 1997.
[13] H.Fischer, "The Persistent Radical Effect: A Principle for Selective Radical Reactions and Living Radical Polymerizations". *Chem. Rev.* vol. 101, pp. 3581-10, 2001.
[14] T.M. Trnka, and R.H. Grubbs, "The Development of L2X2Ru=CHR Olefin Metathesis Catalysts: An Organometallic Success Story*". Acc. Chem. Res.* vol. 34, pp. 18-29, 2001.
[15] J.R.H. Ross, *In Heterogeneous Catalysis: Fundamentals and Applications*. Elsevier, Amsterdam, 2012.
[16] J. Lu, and P.H. Toy, "Organic Polymer Supports for Synthesis and for Reagent and Catalyst Immobilization". *Chem. Rev.* vol. 109, pp.815-38, 2009.
[17] M.Alonzi, M.P.Bracciale, A.Broggi, D.Lanari, A.Marrocchi, M.L.Santarelli, and L. Vaccaro, "Synthesis and characterization of novel polystyrene-supported TBD catalysts and their use in the Michael addition for the synthesis of Warfarin and its analogues". *J. Catal.* vol. 309, pp. 260-67, 2014.
[18] L.Vaccaro, D. Lanari, A.Marrocchi, G. Strappaveccia, "Flow approaches towards sustainability". *Green Chem.* vol. 16 pp. 3680-04, 2014.
[19] T.Angelini, S.Bonollo, D.Lanari, F.Pizzo, and L. Vaccaro, "E-Factor minimized hydrophosphonylation of aldehydes catalyzed by polystyryl-BEMP under solvent-free conditions". *Org. Biomol. Chem.* vol. 11, pp. 5042-46,2013.
[20] S.Bonollo, D. Lanari, T.Angelini, F. Pizzo, A.Marrocchi, and L.Vaccaro, "Rasta resin as support for TBD in base-catalyzed organic processes". *J. Catal.* vol. 285, pp.216-22, 2012.
[21] S. Bonollo, L.Lanari, J.M.Longo, and L. Vaccaro, "E-factor minimized protocols for the polystyryl-BEMP catalyzed conjugate additions of various nucleophiles to a,b-unsaturated carbonyl compounds". *Green Chem.* vol. 14, pp. 164-69, 2012.
[22] R.B. Merrifield, "Solid Phase Peptide Synthesis. I. The Synthesis of a Tetrapeptide". *J. Am. Chem.Soc.* vol. 85, pp. 2149-52, 1963.
[23] E.Zanni, G.De Bellis, M.P. Bracciale, A. Broggi, M.L.Santarelli, , M.S., Sarto, C.Palleschi, , and D.Uccelletti, "Graphite Nanoplatelets and *Caenorhabditis elegans*: Insights from an *in Vivo* Model". *Nano Letters* vol. 12, pp. 2740-44, 2012.
[24] G.S. Mandair, Z. Yu, N. Galaffu, M. Bradley, and A.E. "Russell, Microscopic infrared mapping of chloromethylated polystyrene resin beads". *Appl. Spectroscopy* vol 58, pp. 1282-87, 2004.
[25] K.J.Shea, and G.T. Stoddard, "Chemoselective Targeting of Fluorescence Probes in Polymer Networks. Detection of Heterogeneous Domains in S tyrene-Divinylbenzene Copolymers". *Macromolecules* vol. 24, pp. 1207-09, 1991.
[26] Q.Liu, Y.Li, S.Shen, and Z.Shanshan, "The influence of crosslinking density on the pore morphology of copolymer beads prepared with a novel pore-forming agent". *Mater. Chem. and Phys.* vol. 125, pp. 315-18, 2011.
[27] X.Huanga, N. Qiu, D.Yuan, and B. Huang,. "A novel stir bar sorptive extraction coating based on monolithic material for apolar, polar organic compounds and heavy metal ions". *Talanta* vol. 78, pp.101-06, 2009.
[28] Q.Liu, L.Wang, A. Xiao, H.Yu, Q.Tan, J.Ding, and G. Ren, "Unexpected behavior of 1-chlorodecane as a novel porogen in preparation of high porosity poly(divinylbenzene) microspheres". *J. Phys. Chem. C* vol. 112, pp.13171-74, 2008.
[29] Q.Q. Liu, L.Wang, A.G. Xiao, H.J. Yu, and Q.H. Tan, "A hyper-cross-linked polystyrene with nano-pore structure". *Eur. Polym. J.* vol. 44, pp.2516-22, 2008.
[30] A.K. Nyhus, S.Hagen, and A.Bergej, "Friedel–crafts reactions of pendant vinyl groups in macroporous monosized poly(meta-divinylbenzene) and poly(para-divinylbenzene) particles". *J. Polym. Sci. Polym. Chem.* vol. 38 pp.1366-78, 2000.
[31] O. Okay, "Macroporous copolymer networks". *Progress Polym. Sci.* vol. 25 pp.711-79,2000.
[32] F.S. Macintyre, and D.C. Sherrington, "Control of Porous Morphology in Suspension Polymerized Poly(divinylbenzene) Resins Using Oligomeric Porogens". *Macromolecules* vol. 37, pp. 7628-36, 2004.
[33] M.L.Wang, C.H.Wang, and W. Wang, "Porous macrobeads composed of metal oxide nanocrystallites and with percolated porosity". *J. Mater. Chem.* vol. 17, pp. 2133- 38, 2007.
[34] D.C. Sherrington, "Preparation, structure and morphology of polymer supports". *Chemical Commun.* pp. 2275-86, 1998.
[35] L.Chunling, G.Baojiao, L.Qing, Q. Changsheng, "Preparation of two kinds of chloromethylated polystyrene particle using 1,4-bis (chloromethoxy) butane as chloromethylation reagent". *Colloid Polym. Sci.* vol. 286, pp.553-61, 2008.
[36] U.Wijaya, "Synthesis of Mesoporous Carbons Derived from Hypercrosslinking of Divinylbenzene – 4-Vinylbenzyl Chloride Resin". *IPTEK J. Technol. Sci.* vol. 18, pp.130-362007.
[37] N.Fontanals, J.Cortés, M.Galià, M.R. Mercè, P.A.G Cormack, F. Borrull, D.C. Sherrington, "Synthesis of Davankov-Type Hypercrosslinked Resins Using Different Isomer Compositions of Vinylbenzyl Chloride Monomer, and Application in the Solid-Phase Extraction of Polar Compounds". *J. Polym.Sci. Polym. Chem.* vol. 43, pp. 1718-28. 2005.
[38] S.Subramonian, "Anion-exchange resins from vinylbenzyl choride: control of hydrolysis during polymerization". *React. Funct. Polym.* vol. 29, pp. 129-33, 1996.
[39] R.V. Law, D.C. Sherrington, C.E. Snape, I.Ando, H. Kurosu, "Solid-State 13C MAS NMR Studies of Hyper-Cross-Linked Polystyrene Resins". *Macromolecules*. vol. 29, pp. 6284-93,1996.
[40] M.H.Mohamed, and L.D. Wilson, "Porous Copolymer Resins: Tuning Pore Structure and Surface Area with Non Reactive Porogens". *Nanomater*. vol. 2, pp.163-86, 2012.
[41] D.X. Hao, F. L.Gong, W.Wei, G.H. Hu, G.H.Ma, and Z.G. Su, "Porogen effects in synthesis of uniform micrometer-sized poly(divinylbenzene) microspheres with high surface areas". *J. Colloid Interf. Sci.* vol. 323, pp. 52-59, 2008.

Supporting information for

Preparation and characterization of cross-linked polymer supports for catalysts immobilization

Maria P. Bracciale[1], Alessandra Broggi[2*], Elena Bartollini[3], Francesca Sbardella[4], Matteo Poldi[5], Assunta Marrocchi[6*], Maria L. Santarelli[7*], Luigi Vaccaro[8*]

[1,2,4,5,7]Dipartimento di Ingegneria Chimica Materiali Ambiente, Università di Roma "La Sapienza", Via Eudossiana 18, 00185 Roma, Italy; [3,6,8]Laboratory of Green Synthetic Organic Chemistry, Dipartimento di Chimica, Università degli Studi di Perugia, Via Elce di Sotto 8, 06123 Perugia, Italy.

e-mail: alessandra.broggi@uniroma1.it; assunta.marrocchi@unipg.it; marialaura.santarelli@uniroma1.it; luigi.vaccaro@unipg.it

General procedure for the preparation of chloromethylated resins PS-Cl 1*b-o*

PS-Cl 1b. Prepared by following the procedure described in the Experimental Section, Main Text, for **1*a***. Stabilizer: poly(vinyl alcohol) (MW 85,000–124,000, 99% hydrolyzed) (0.4%) (yield 75%).

PS-Cl 1c. Prepared by following the procedure described in the Experimental Section, Main Text, for **1*a***. Stabilizer: poly(vinyl alcohol) (MW 13,000-23,000, 99% hydrolyzed) (0.1%) (yield 68%).

PS-Cl 1d. Prepared by following the procedure described in the Experimental Section, Main Text, for **1*a***. Stabilizer: poly(vinyl alcohol) (MW 13,000-23,000, 99% hydrolyzed) (0.4%) (yield 70%).

PS-Cl 1e **.** Prepared by following the procedure described in the Experimental Section, Main Text, for **1*a***. Porogen: cyclohexanol (COX); Stabilizer: poly(vinyl alcohol) (MW 13,000-23,000, 99% hydrolyzed) (0.1%) (yield 65%).

PS-Cl 1f. Prepared by following the procedure described in the Experimental Section, Main Text, for **1*a***. Porogen: cyclohexanol (COX); Stabilizer: poly(vinyl alcohol) (MW 85,000–124,000, 99% hydrolyzed) (0.1%) (yield 70%).

PS-Cl 1g. Prepared by following the procedure described in the Experimental Section, Main Text, for **1*a***. Porogen: cyclohexanol (COX); Stabilizer: poly(vinyl alcohol) (MW 85,000–124,000, 99% hydrolyzed) (0.4%) (yield 71%).

PS-Cl 1h. Prepared by following the procedure described in the Experimental Section, Main Text, for **1*a***. Porogen: cyclohexanol (COX); Stabilizer: poly(vinyl alcohol) (MW 85,000–124,000, 99% hydrolyzed) (0.4%); VBC/S/DV: 0.6/0.2/0.2 (yield 68%).

PS-Cl 1i. Prepared by following the procedure described in the Experimental Section, Main Text, for **1*a***. Porogen: cyclohexanol (COX); Stabilizer: poly(vinyl alcohol) (MW 85,000–124,000, 99% hydrolyzed) (0.4%); VBC/S/DV: 0.6/0 /0.4 (yield 73%).

PS-Cl 1j. Prepared by following the procedure described in the Experimental Section, Main Text, for **1*a***. Porogen: cyclohexanol (COX); Stabilizer: poly(vinyl alcohol) (MW 13,000-23,000, 99% hydrolyzed) (0.4%) (yield 65%).

PS-Cl 1k. Prepared by following the procedure described in the Experimental Section, Main Text, for **1*a***. Porogen: 1-chlorodecane (1-CD); Stabilizer: poly(vinyl alcohol) (MW 85,000–124,000, 99% hydrolyzed) (0.1%) (yield 71%).

PS-Cl 1l. Prepared by following the procedure described in the Experimental Section, Main Text, for **1*a***. Porogen: 1-chlorodecane (1-CD); Stabilizer: poly(vinyl alcohol) (MW 85,000–124,000, 99% hydrolyzed) (0.4%) (yield 68%).

PS-Cl 1m. Prepared by following the procedure described in the Experimental Section, Main Text, for **1*a***. Porogen: 1-

chlorodecane (1-CD); Stabilizer: poly(vinyl alcohol) (MW 85,000–124,000, 99% hydrolyzed) (0.4%); VBC/S/DV: 0.4/0.4/0.2 (yield 75%).

PS-Cl 1n. Prepared by following the procedure described in the Experimental Section, Main Text, for **1*a***. Porogen: 1-chlorodecane (1-CD); Stabilizer: poly(vinyl alcohol) (MW 13,000-23,000, 99% hydrolyzed) (0.4%) (yield 70%).

PS-Cl 1o. Prepared by following the procedure described in the Experimental Section, Main Text, for **1*a***. Porogen: 1-chlorodecane (1-CD); Stabilizer: poly(vinyl alcohol) (MW 13,000-23,000, 99% hydrolyzed) (0.1%) (yield 70%).

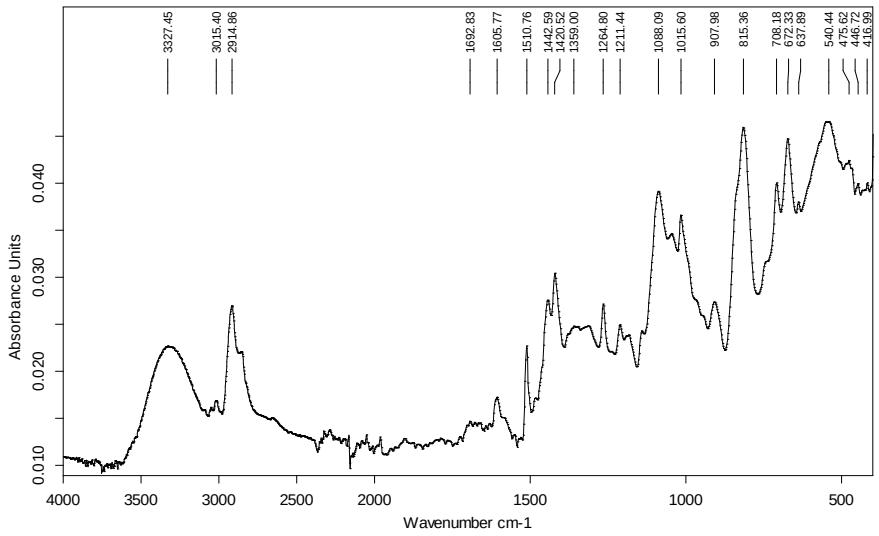

FIGURE SI1. FTIR ANALYSIS OF POLYMER 1b.

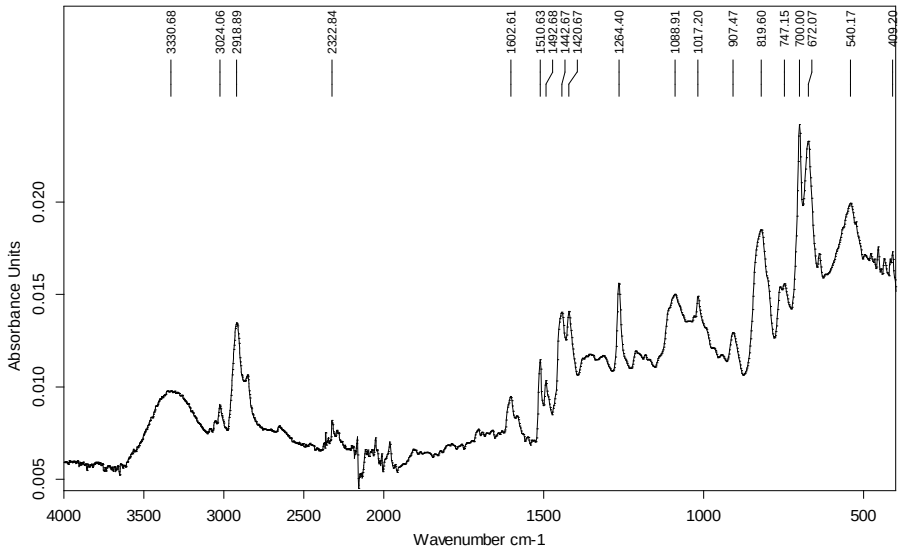

FIGURE SI2. FTIR ANALYSIS OF POLYMER 1h.

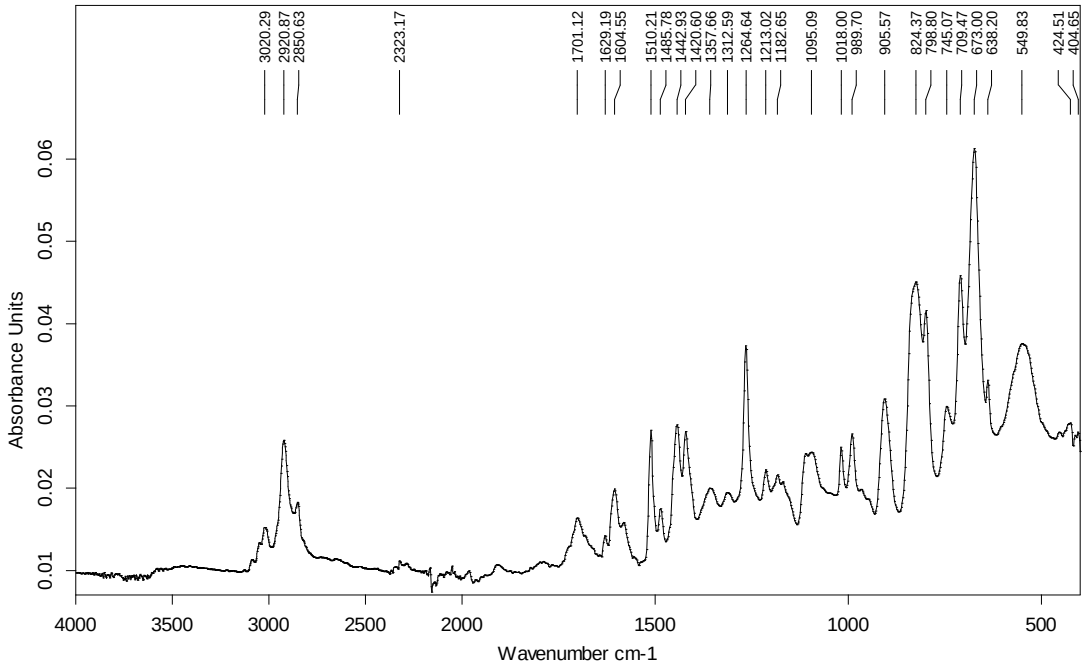

FIGURE SI3. FTIR ANALYSIS OF POLYMER 1i.

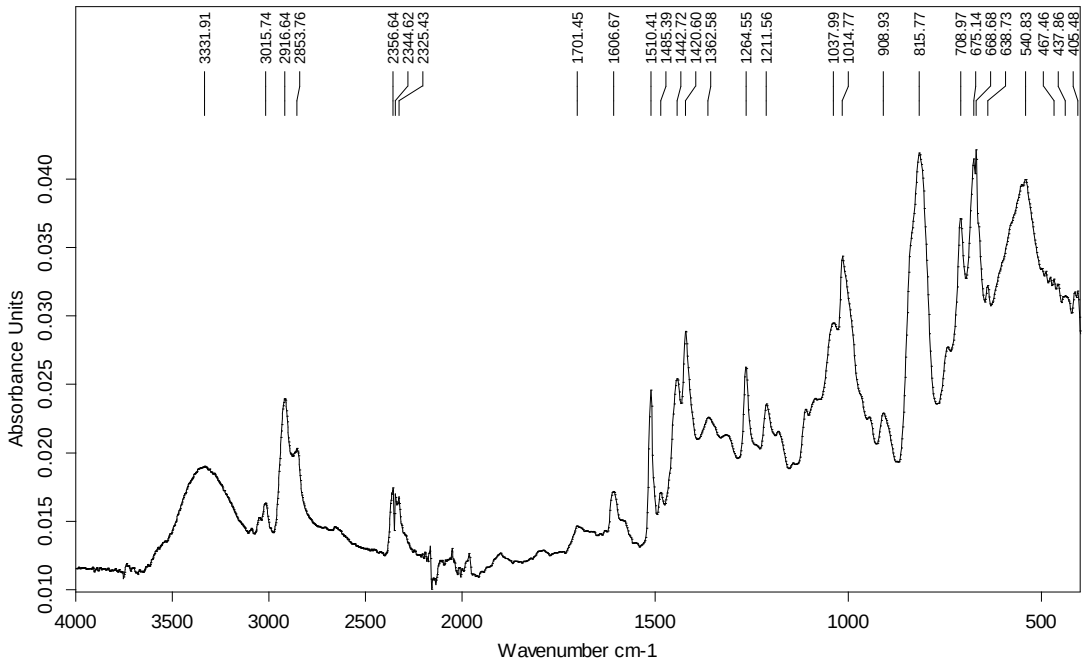

FIGURE SI4. FTIR ANALYSIS OF POLYMER 1*j*.

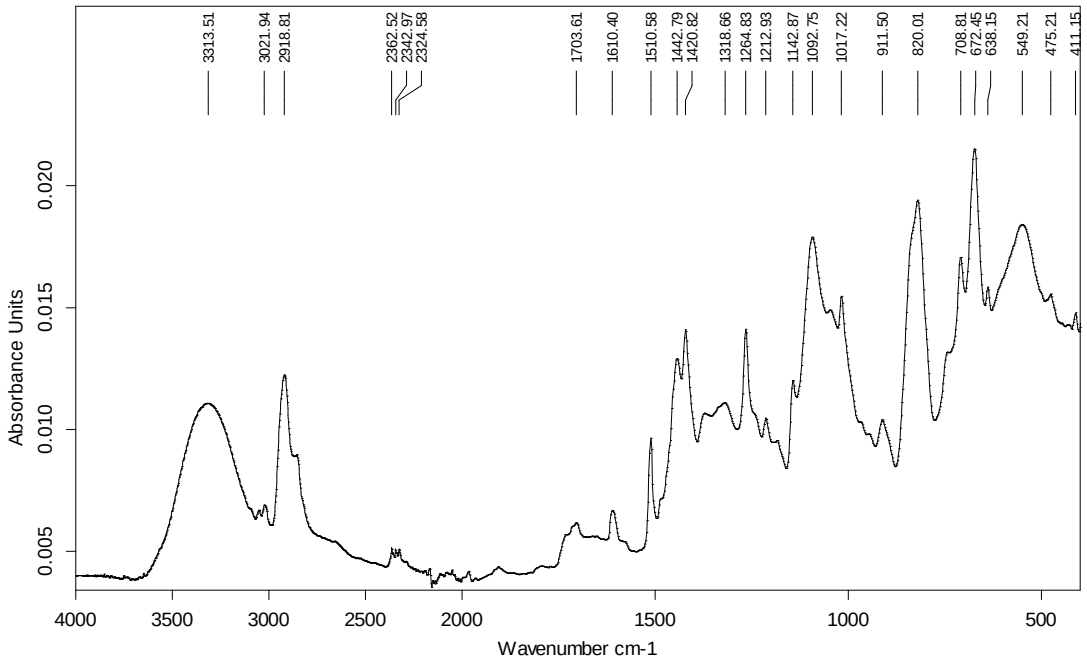

FIGURE SI5. FTIR ANALYSIS OF POLYMER 1*l*.

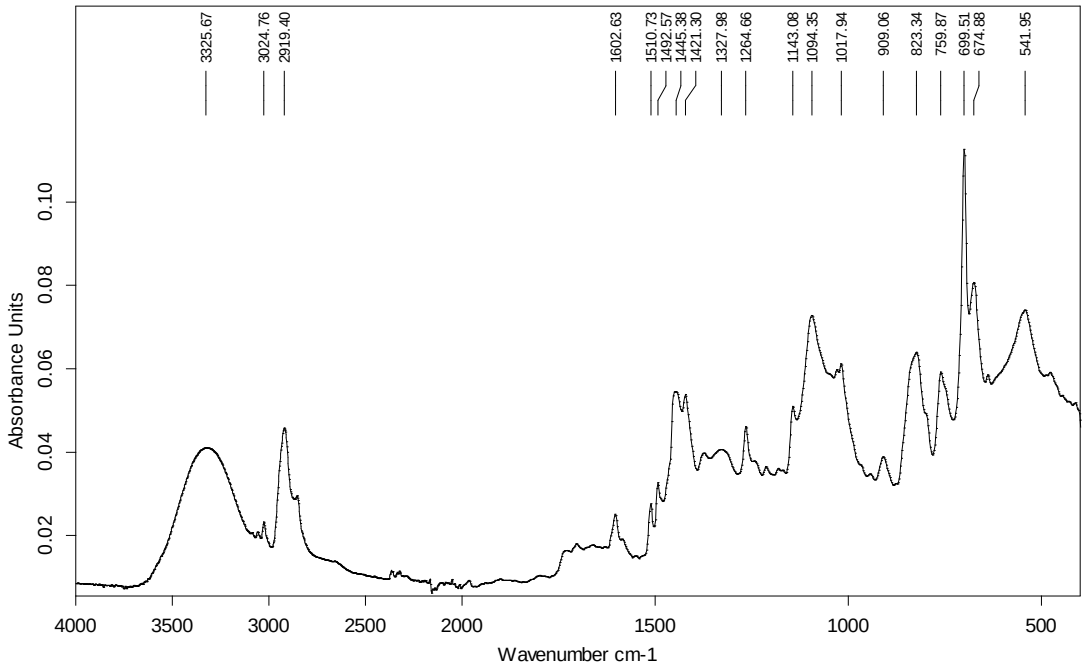

FIGURE SI6. FTIR ANALYSIS OF POLYMER 1*m*.

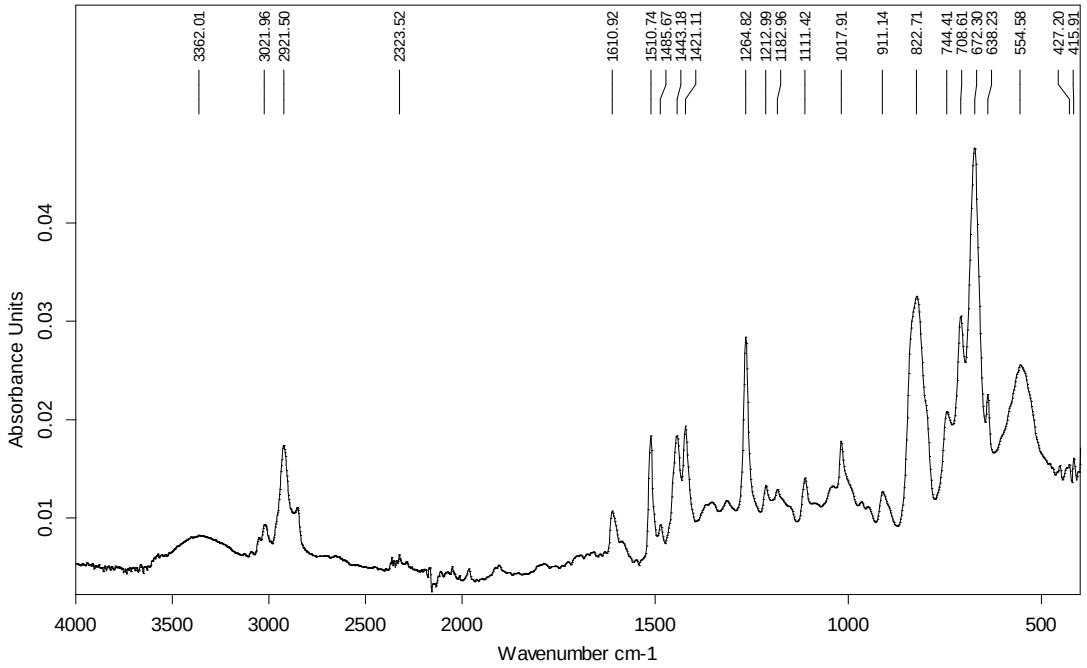

FIGURE SI7. FTIR ANALYSIS OF POLYMER 1*o*.

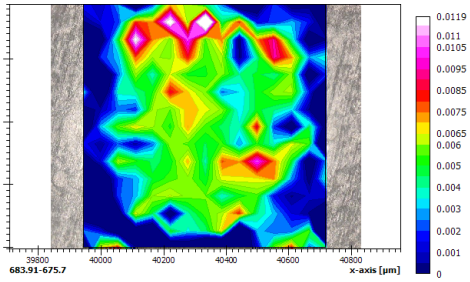

(a) Resin **1b**

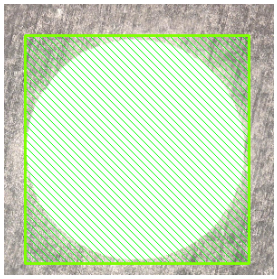

(f) Resin **1b**

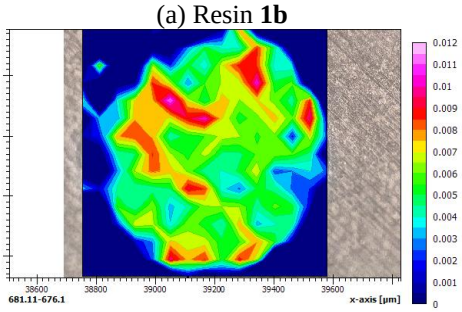

(b) Resin **1h**

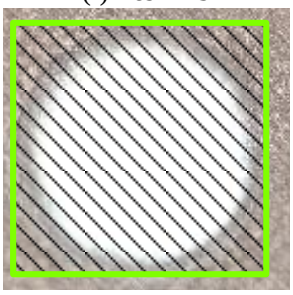

(g) Resin **1h**

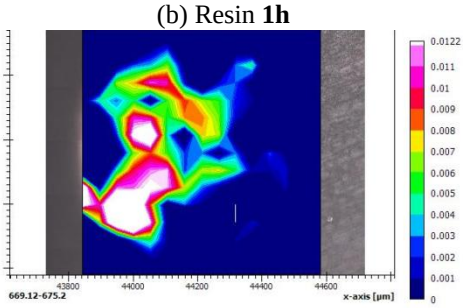

(c) Resin **1j**

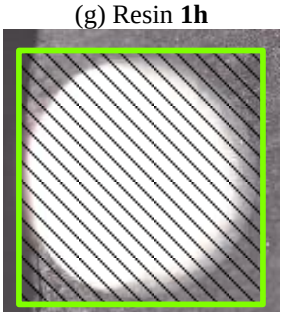

(h) Resin **1j**

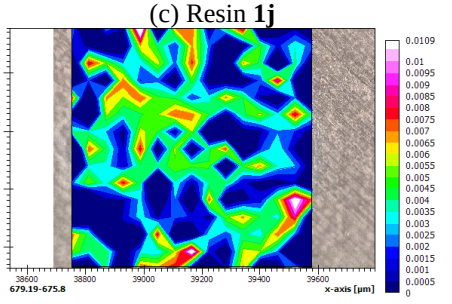

(d) Resin **1l**

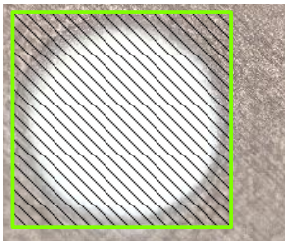

(i) Resin **1l**

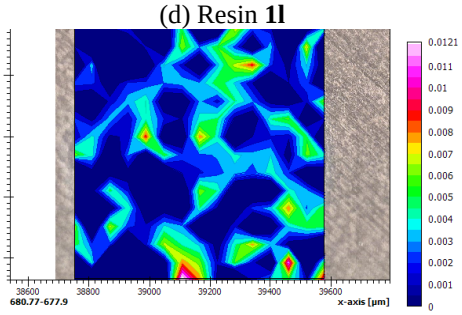

(e) Resin **1m**

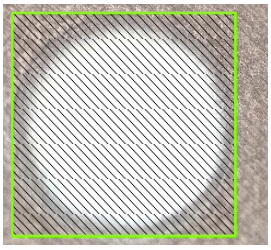

(j) Resin **1m**

FIGURE SI8. SPECTROSCOPIC 2D IMAGES OF THE SPATIAL DISTRIBUTION OF–Cl GROUPS (A-E). OPTICAL MICROSCOPY IMAGES 15X (F-J) SHOWING THE HALF-CUT BEAD MAPPING TRACE.

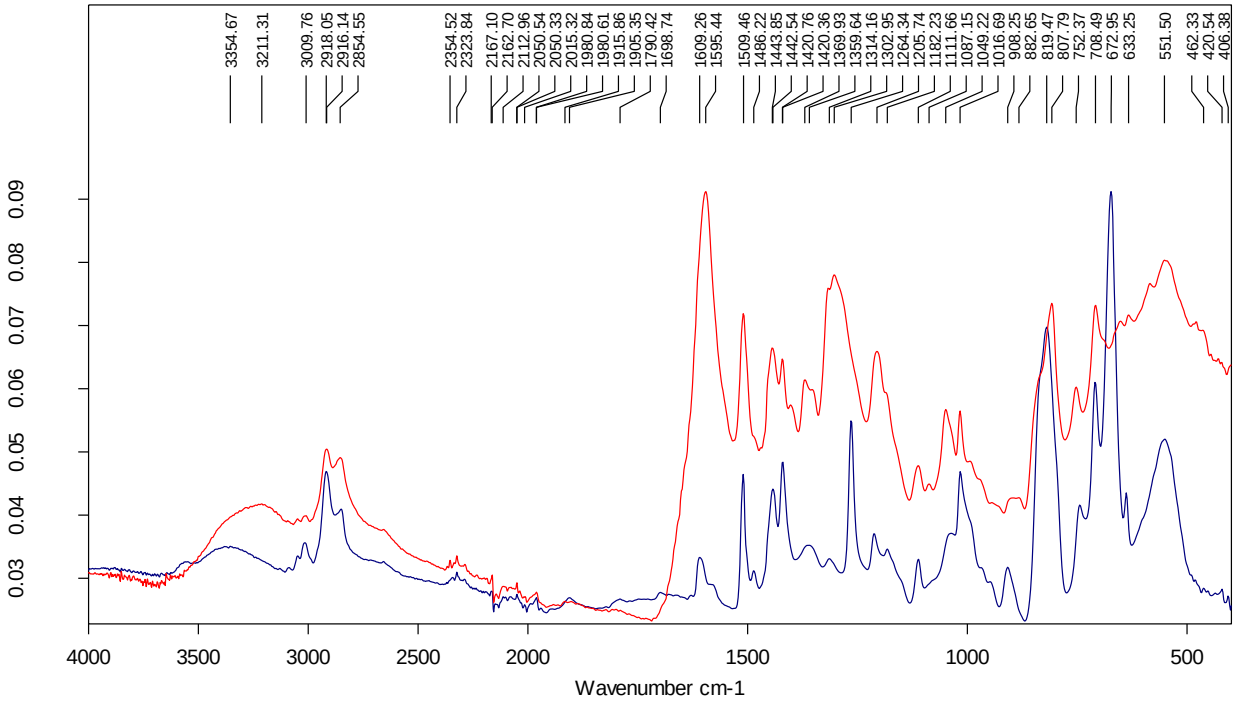

FIGURE SI9. FTIR ANALYSIS OF POLYMER 1l (BLU LINE) AND 1l AFTER NUCLEOPHILIC SUBSTITUTION OF THE CHLORINE ATOMS BY 1,5,7-TRIAZABICYCLO[4.4.0]DEC-5-ENE (TBD) (RED LINE).

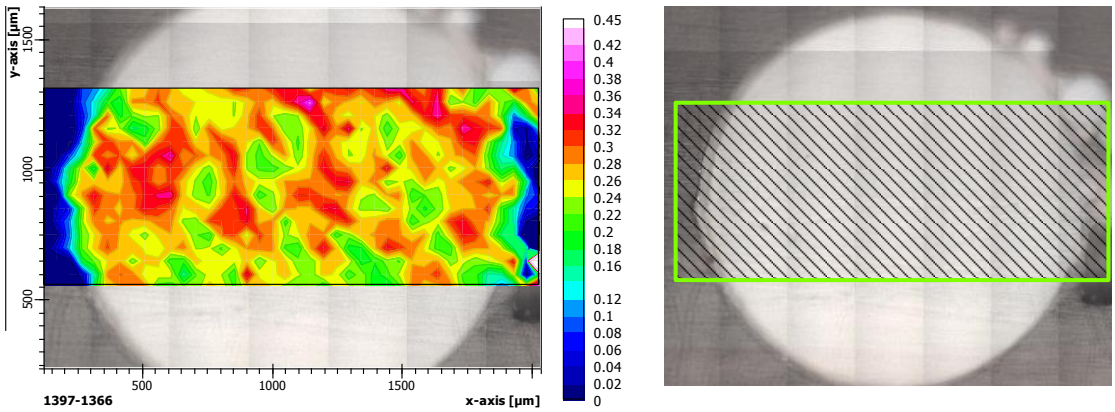

(a) (b)

FIGURE SI10. SPECTROSCOPIC 2D IMAGE OF THE SPATIAL DISTRIBUTION OF –TBD GROUP (A). OPTICAL MICROSCOPY IMAGE 15X (B) SHOWING THE HALF-CUT BEAD MAPPING TRACE.

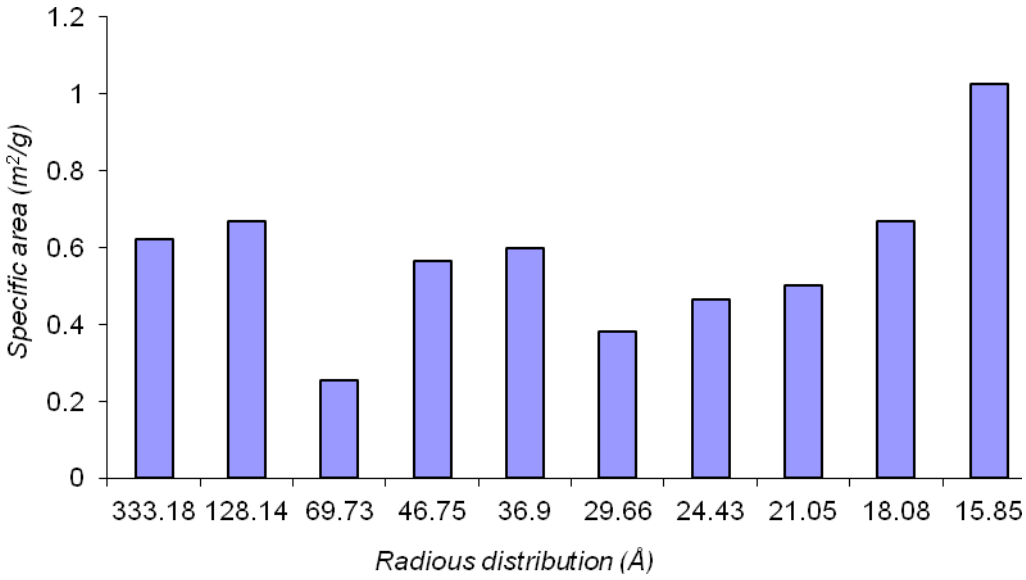

FIGURE SI11. PORE SIZE DISTRIBUTION OF POLYMER 1a.

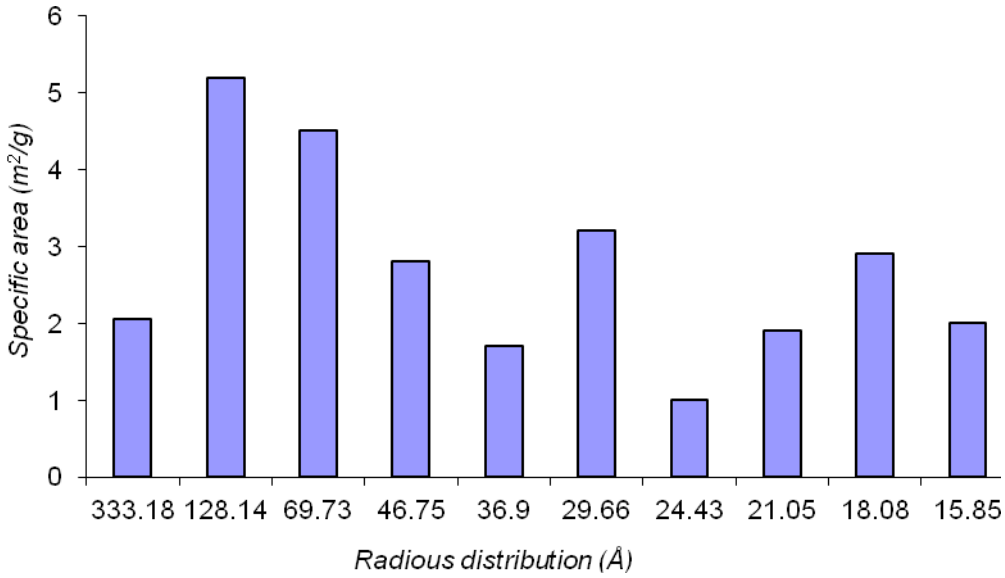

FIGURE SI12. PORE SIZE DISTRIBUTION OF POLYMER 1b.

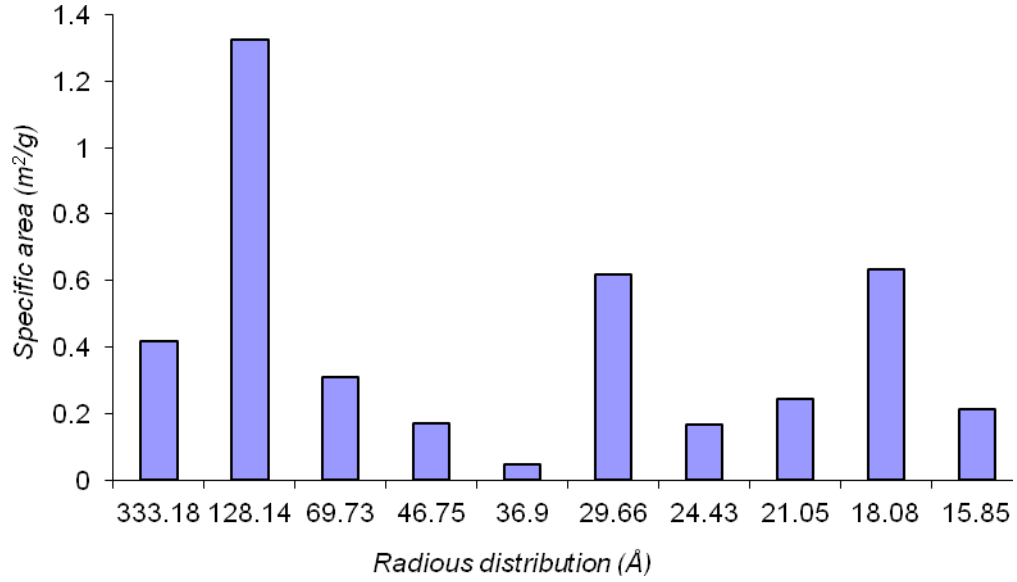

FIGURE SI13. PORE SIZE DISTRIBUTION OF POLYMER 1h.

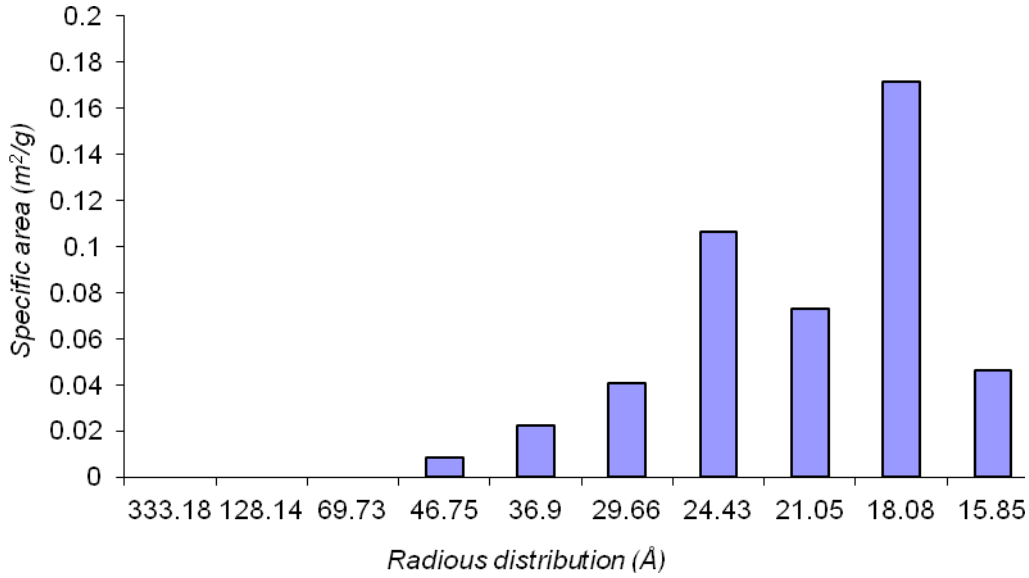

FIGURE SI14. PORE SIZE DISTRIBUTION OF POLYMER 1i.

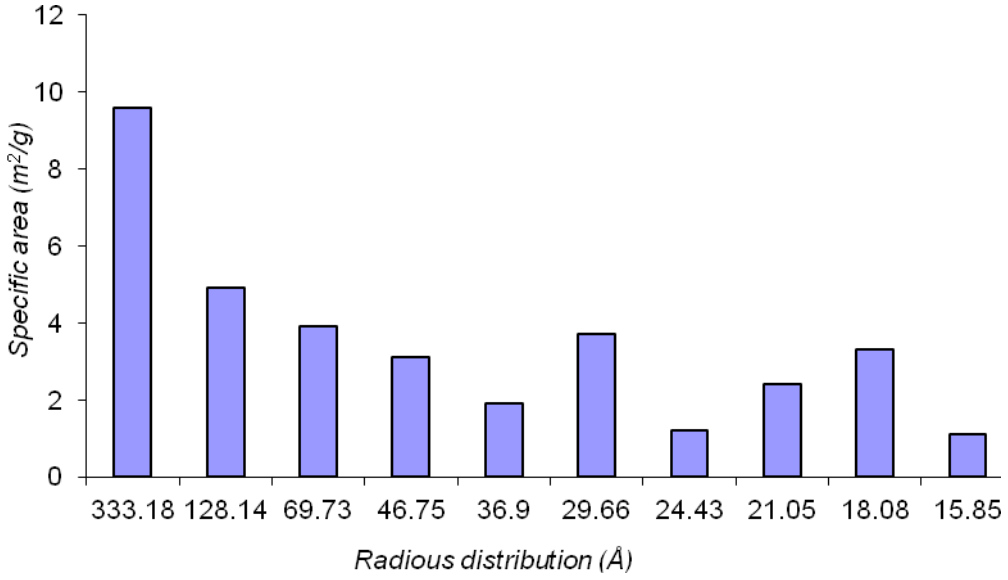

FIGURE SI15. PORE SIZE DISTRIBUTION OF POLYMER 1j.

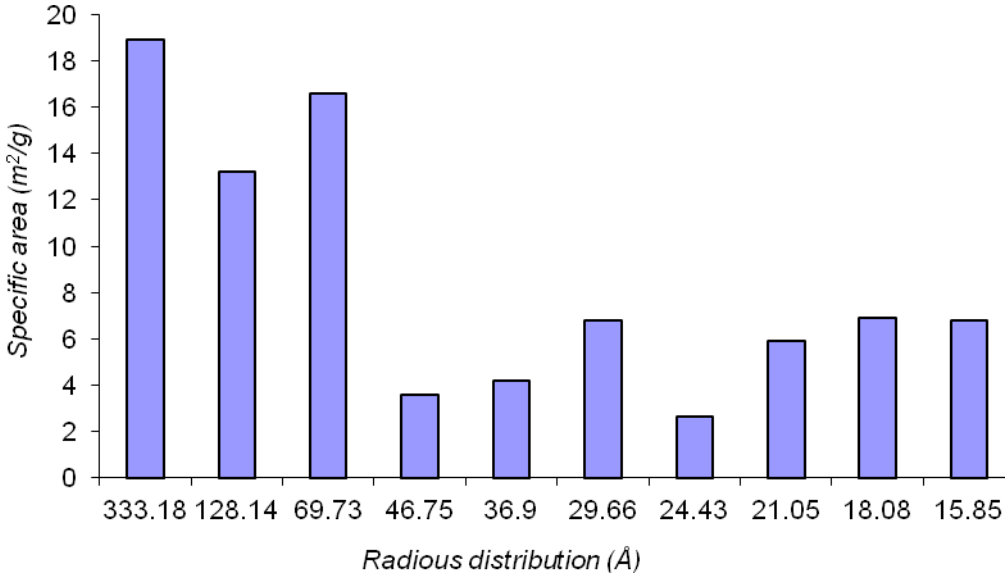

FIGURE SI16. PORE SIZE DISTRIBUTION OF POLYMER 1l.

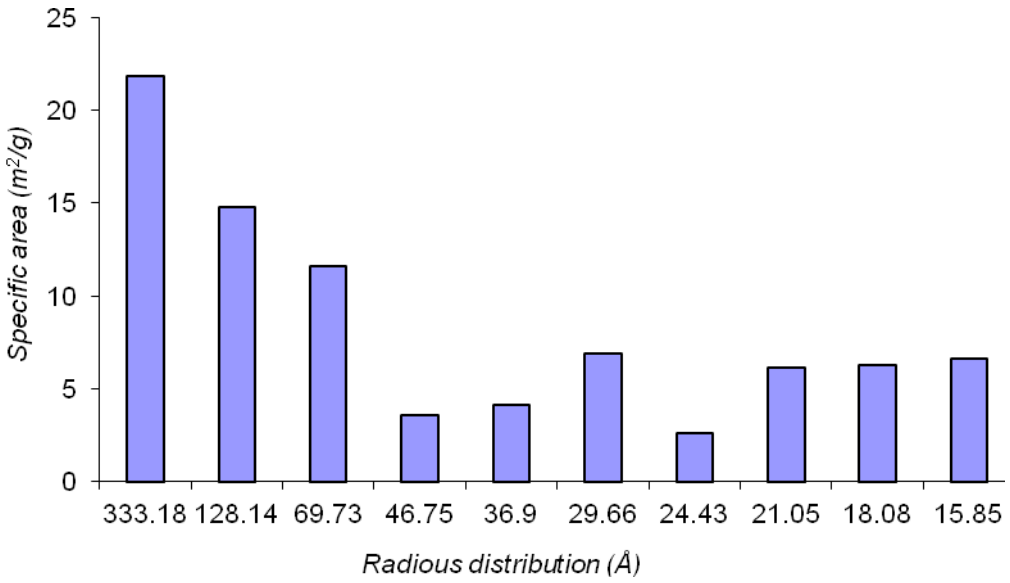

FIGURE SI17. PORE SIZE DISTRIBUTION OF POLYMER 1m.

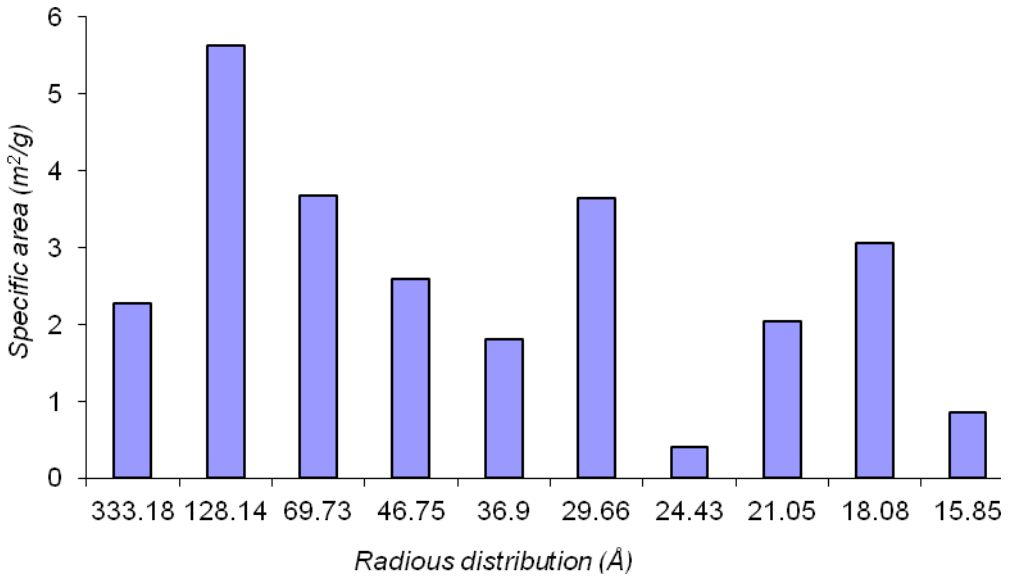

FIGURE SI18. PORE SIZE DISTRIBUTION OF POLYMER 1n.

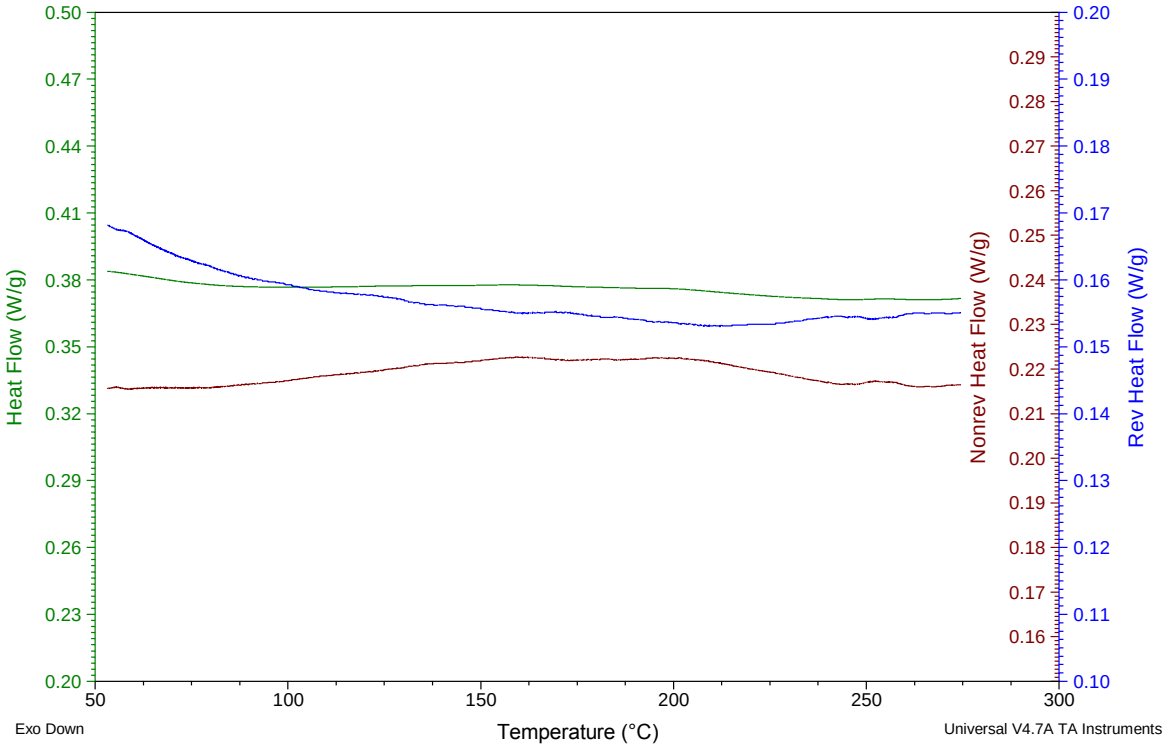

FIGURE SI19. MTDSC ANALYSIS OF POLYMER 1a.

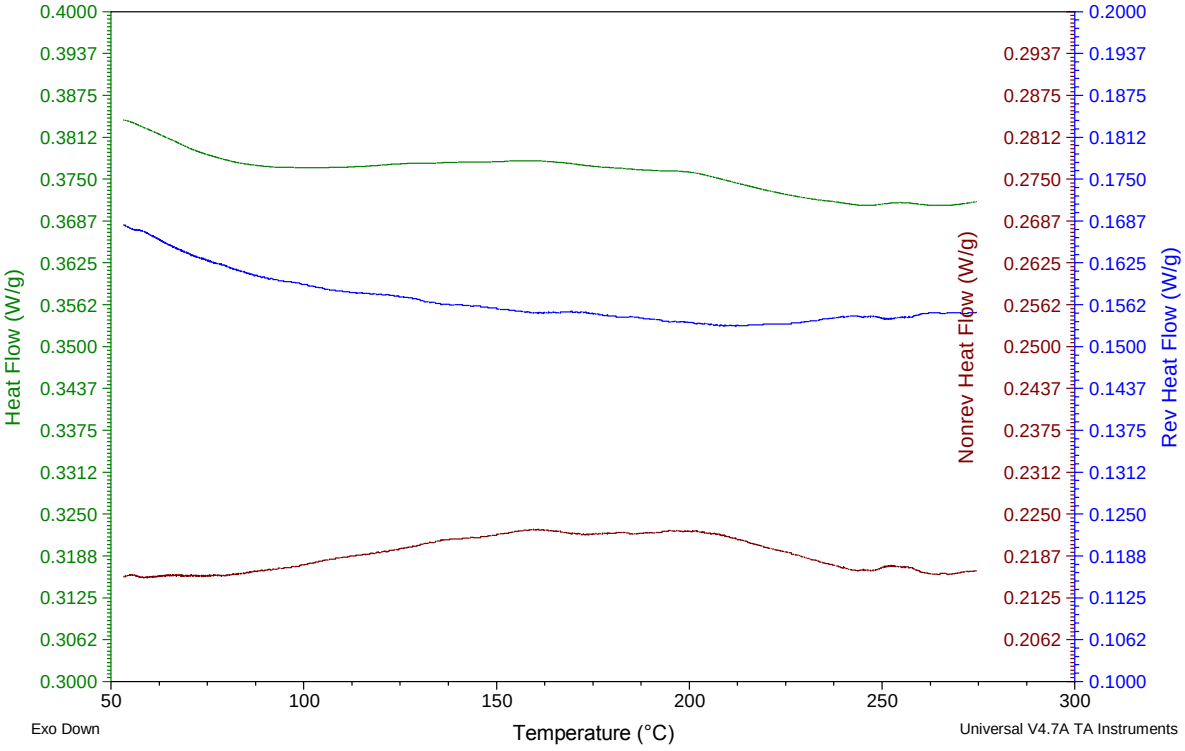

FIGURE SI20. MTDSC ANALYSIS OF POLYMER 1b.

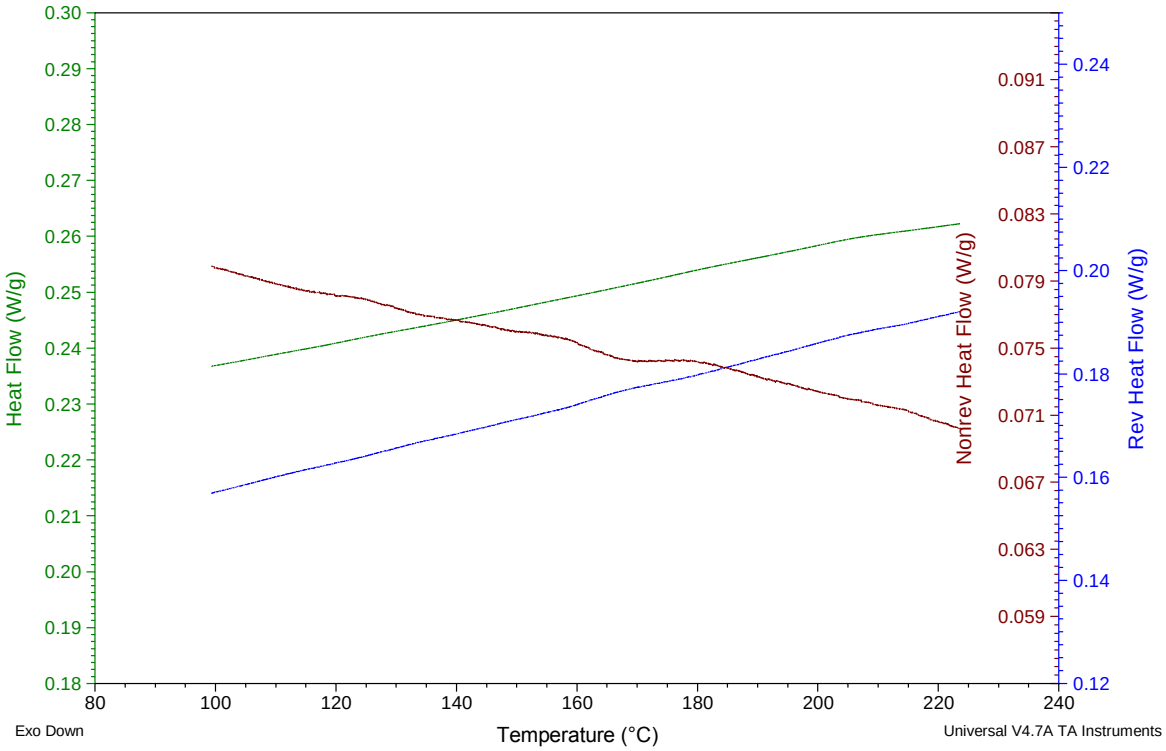

FIGURE SI21. MTDSC ANALYSIS OF POLYMER 1h.

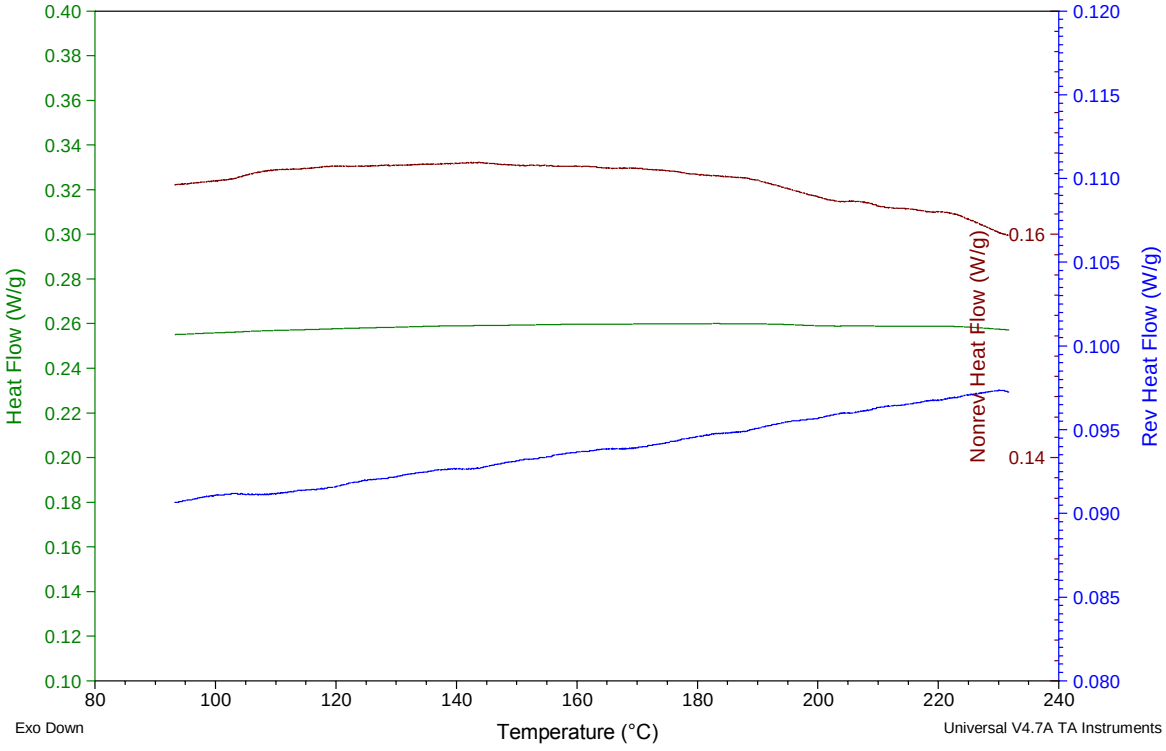

FIGURE SI22. MTDSC ANALYSIS OF POLYMER 1i.

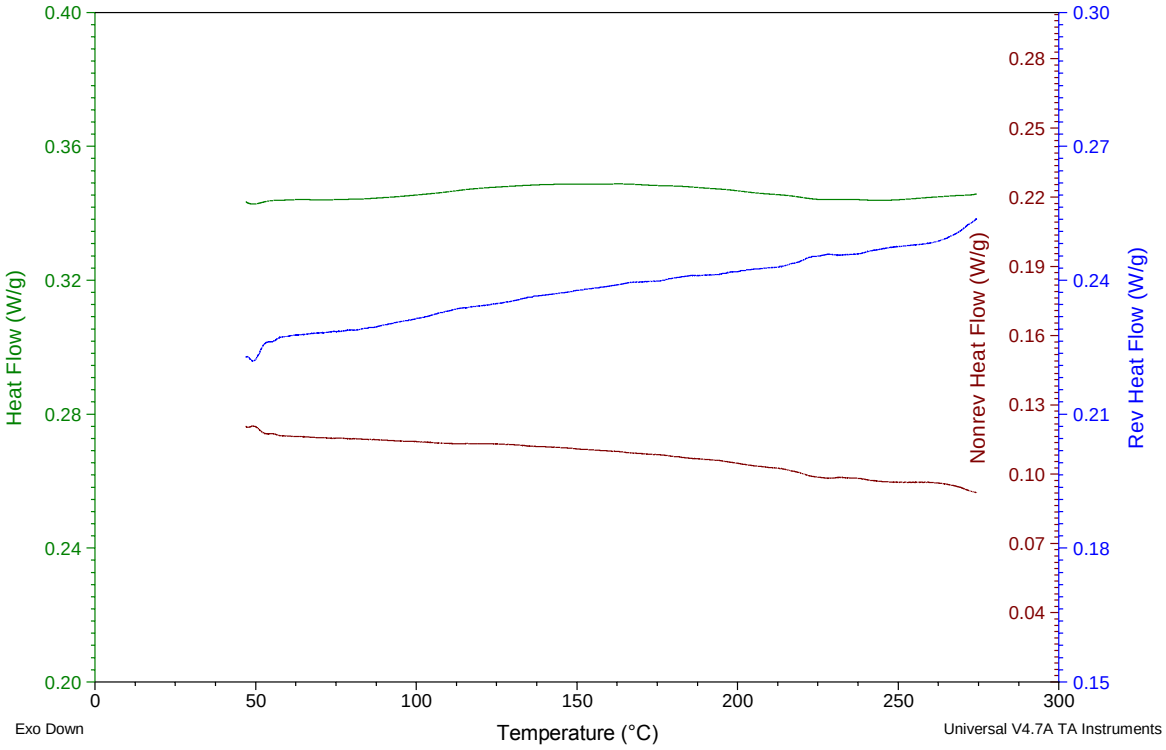

FIGURE SI23. MTDSC ANALYSIS OF POLYMER 1j.

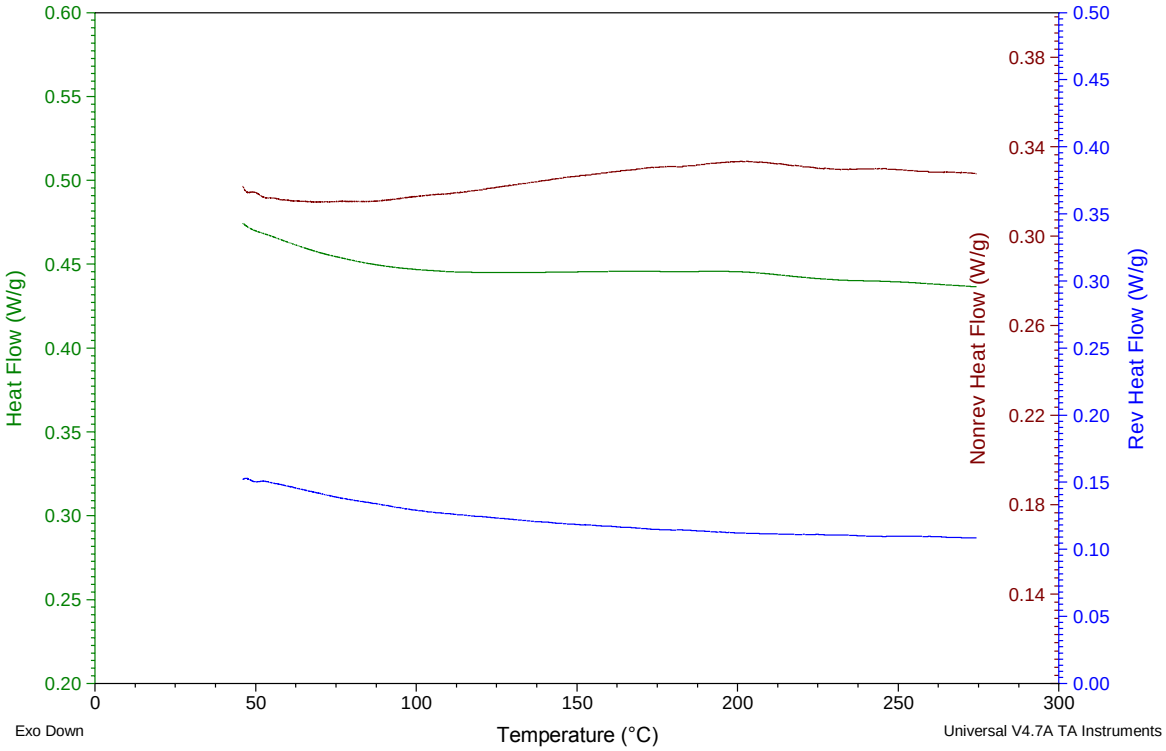

FIGURE SI24. MTDSC ANALYSIS OF POLYMER 1l.

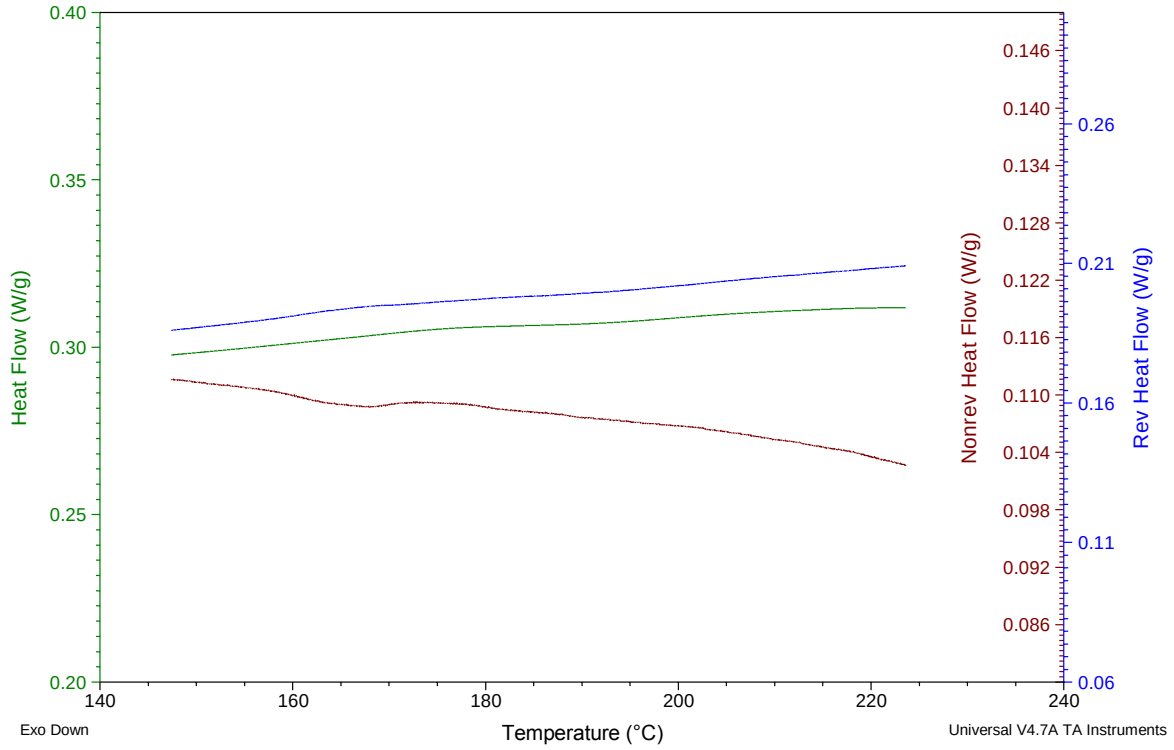

FIGURE SI25. MTDSC ANALYSIS OF POLYMER 1m.

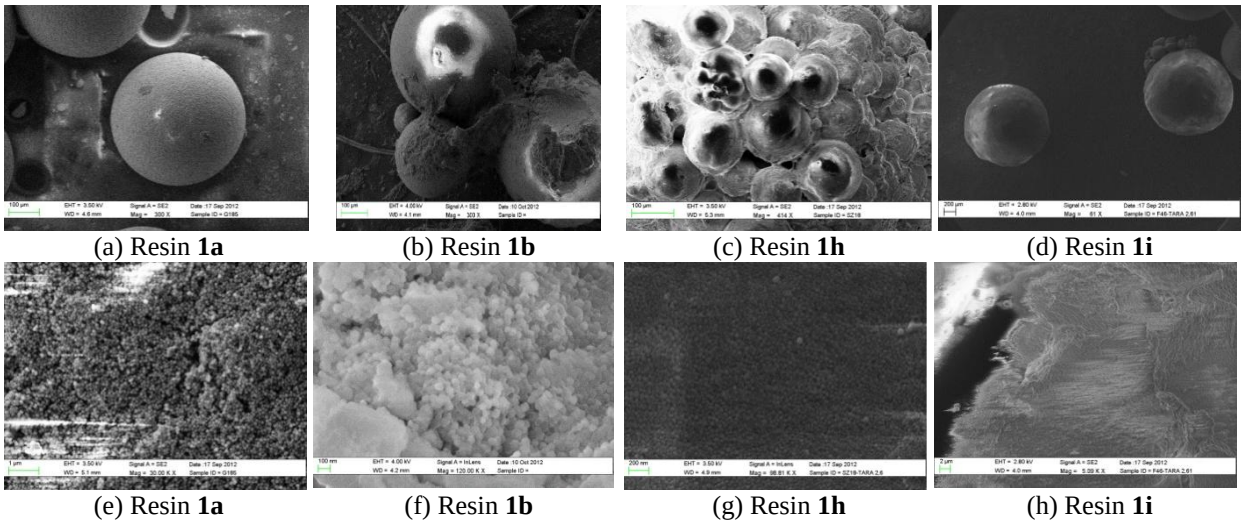

(a) Resin **1a** (b) Resin **1b** (c) Resin **1h** (d) Resin **1i**

(e) Resin **1a** (f) Resin **1b** (g) Resin **1h** (h) Resin **1i**

FIGURE SI26. SCANNING ELECTRON MICROSCOPY IMAGES OF RESINS BEADS PREPARED BY USING (A,B) 2-EHA POROGEN, (C,D) COX POROGEN, AND THE CORRESPONDING MACROPOROUS RESIN FRACTURES (E-H).

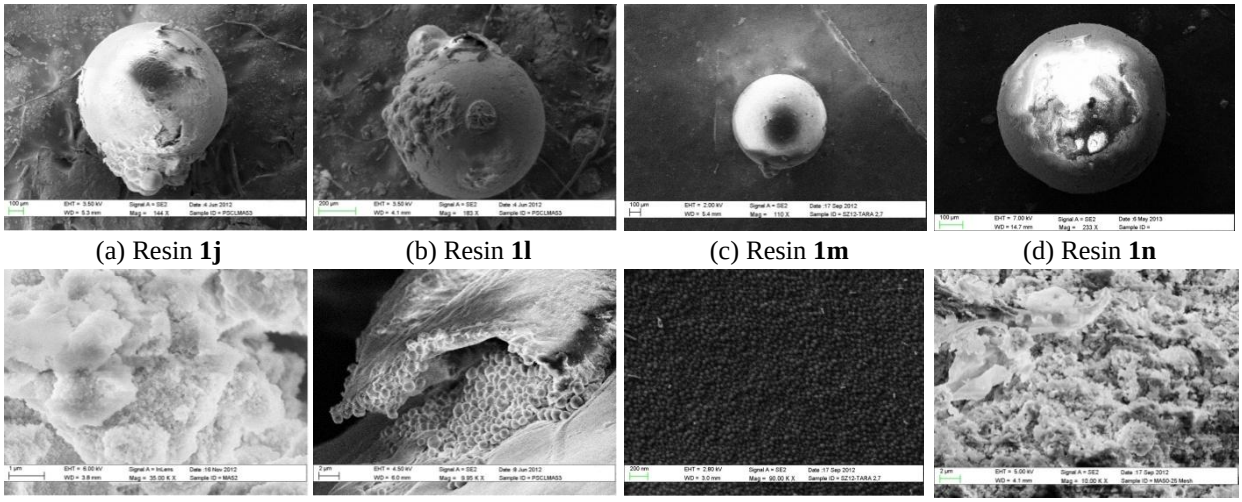

(a) Resin **1j** (b) Resin **1l** (c) Resin **1m** (d) Resin **1n**

(e) Resin **1j** (f) Resin **1l** (g) Resin **1m** (h) Resin **1n**

FIGURE SI27. SCANNING ELECTRON MICROSCOPY IMAGES OF RESINS BEADS PREPARED BY USING (A) COX POROGEN, (B,C,D) 1-CD POROGEN, AND THE CORRESPONDING MACROPOROUS RESIN FRACTURES (E-H).